Progress In Electromagnetics Research B, Vol. 97, 167–197, 2022

Critical Analysis of the Recent Trends and Advancements in Dielectric Resonator Antennas

Shailza Gotra[1, *] and Vinay S. Pandey[2]

Abstract—A comprehensive overview of dielectric resonator antenna (DRA) is presented in this paper. Several techniques have been reported in the literature for the performance improvement of DRA. Over the past few decades, circularly polarized (CP) DRAs have been widely explored to mitigate multipath fading and polarization losses in comparison to linearly polarized (LP) antennas. Apart from this, high data transfer rate is required, which needs the development in the field of multi-input-multi-output (MIMO) antenna designs. This includes the increase in the channel capacity without exploiting the limited constraints like signal power and bandwidth. Thus, exploring the concept of MIMO in DRA along with the diversity performance features leads to the development in this field. Furthermore, to mitigate the conduction losses at THz and optical frequencies, high-efficiency DRA proves rationale in extending towards the higher frequency ranges. These scintillating features pave the path for efficient devices integration and on-chip applications at higher frequency ranges where the performance of metallic radiator degrades. Also, the dispersive properties of metal conductivity lead to plasmonic behaviour resulting in the dissipation losses at the optical frequencies. These losses can be substantially mitigated using DRAs. This can be efficiently realized for the future application that requires the manipulation of high-resolution light.

1. INTRODUCTION

The theoretical development of dielectric resonator (DR) in the context of microwave devices like filters, oscillators, and resonators was stated back in the late 1939 by Ritchmyer [1]. It demonstrated the concept of DR radiations in open environment. A DR consists of a non-metallic resonator made up of high-quality factor (Q-factor) dielectric material used for the design of microwave circuit elements. In 1962, Okaya and Barash studied the first and second-order approximations of the resonant frequencies for investigating modes of oscillations inside the DR. This study investigated the band-pass and band-reject filters using a DR in the form of crystal [2]. Later, extensive theoretical and experimental analysis of high Q-factor DR as the filters was performed [3]. In 1968, Sager and Tisi reported the eigen modes and forced resonant modes of a spherical DR in their study [4]. This investigation was carried out with two practical aims. One used a high Q-factor DR for waveguide applications, and the other included matching with the low-impedance short dipole antenna. It was found that in both the cases, discrete resonances occur for the different ratios of radius to wavelength of the sphere. Further, it was reported that TM_{mnp} and TE_{mnp} modes existed, when being excited by the short electric and magnetic dipoles, respectively. Van Bladel, in 1975, presented a detailed theory for the evaluation of confined and non-confined modes inside a high-permittivity DR [5, 6]. In 1980, Kobayashi and Tanaka studied the resonant modes of a dielectric rod resonator and generalized the modes as leaky and trapped states [7]. Initially, the DRs were shielded inside the metallic cavities to maintain the high Q-factor. Thus, DRs

Received 23 September 2022, Accepted 14 November 2022, Scheduled 7 December 2022
* Corresponding author: Shailza Gotra (shailzagotra@outlook.com).
[1] Department of Electronics and Communication Engineering, Indian Institute of Technology Roorkee, India. [2] Department of Applied Sciences, National Institute of Technology Delhi, India.

were utilized for the conventional applications like filters and oscillators. However, the use of DR as the radiator in antenna designs was not addressed until then apart from the proof of radiations in open environment for a long time.

The first experimental investigation of cylindrical DR cavity antenna was reported by Long and McAllister in 1983 [8]. Subsequently, they investigated rectangular and hemispherical DRs in 1983 and 1984, respectively, as the radiating element of the antenna [9, 10]. Apart from this, various shapes of DR were analysed including ring [11], triangle [12], and sphere [13] along with the study of radiation characteristics and different applications. A broadband stacked cylindrically shaped dielectric resonator antenna (DRA) was reported with the coaxial feeding technique [14]. The use of differently shaped DRAs with proper excitation techniques have been explored by many researchers over the decades. A cylindrical DRA was reported with the microstrip transmission line excitation for investigating the coupling behaviour and radiation characteristics [15]. A coplanar waveguide feeding mechanism was reported in a cylindrical DRA [16]. A hemispherical DRA was reported with the coaxial feeding technique for the study of input impedance [17]. A stacked annular ring was reported using the axisymmetric coaxial probe excitation [18]. In 1991, St-Martin et al. reported an aperture-coupled cylindrical DRA [19]. The aperture-coupled excitation technique consists of a slot in metallic ground plane through which field leaked in the DR structure to define the specific modes. In 1996, Antar and Fan theoretically investigated the aperture-coupled feeding technique in a rectangular DRA [20]. A half-split cylindrical DR was reported with the slot-coupling technique excited as the magnetic dipole mode [21]. The rigorous theories for the evaluation of modes in the DR with respect to the radiated field analysis were studied and investigated [22, 23]. In 1993, Kishk et al. computed the resonant frequencies and far-field characteristics of isolated DR disc. This study evaluated the expressions for resonant frequency and Q-factor and dependence on disc dimensions using curve-fitting technique [24]. The radiation efficiency of a DRA was experimentally investigated over the theoretical considerations [25]. Kishk with his colleagues numerically computed the radiation characteristics of a cylindrical DRA excited using the coaxial feeding technique [26]. In 1994, Mongia and Bhartia reported a comprehensive study on the transverse electric (TE), transverse magnetic (TM) and hybrid electromagnetic (HEM) modes existence and radiation field characteristics of different DR geometries [27].

This review study derives the accurate closed form expression that provides an insight of the relation among the resonant frequency, Q-factor, and bandwidth of the antenna. The advancements in the field of DRA with respect to numerous shapes of DR, feeding techniques, radiation characteristics, and mode analysis have been investigated and reported [30, 31]. The concept of utilizing the high-efficiency DRAs has not been limited to microwave and millimetre wave applications. Consequently, researchers have explored the concept of nanoantenna at THz, optical, visible, and infrared frequency regions [32]. At higher frequency ranges, the conventional conducting radiator loses its electronic properties due to various losses [33]. To mitigate these losses, silicon based dielectric resonators [28, 34, 35], graphene-based radiators [36, 37], vanadium dioxide based radiators [38], and various other materials have come up as the suitable futuristic approach in the field of antenna designing. However, high efficiency silicon based DRAs have gained the focus of various researchers due to the advantage of low conduction losses and high resistivity material having highly stable permittivity at THz frequencies [39]. These scintillating features of nano-DRAs can be efficiently utilized for devices integration and on-chip applications at higher frequency ranges where the performance of metallic radiator degrades. Also, the dispersive properties of the metal conductivity lead to the plasmonic behaviour resulting in the dissipation losses at the optical and infrared frequencies. These losses can be substantially mitigated using DRAs. Thus, it can be efficiently realized for the future nanophotonics applications that require the manipulation of high-resolution light. Fig. 1 shows the simulated silicon-based NDRA geometry with side view [28] and dielectric rod NDRA and image of the fabricated prototype of the antenna at optical frequencies [29]. It shows the scope of the modelling and fabrication of the NDRA at the THz and optical frequency regime. Sethi et al. have reported a nano-DRA (NDRA) for integration with the standard 1550 nm optical communication systems [35]. An NDRA has been reported for nanophotonics applications at S, C, and L-bands of the optical spectrum [40]. The efficiency and scaling behaviour of DRA have been studied at optical frequencies by Zou et al. [41]. Zou and his colleagues have reported an NDRA at visible frequencies [42]. Consequently, these developments lead to the emphasis on the improvements in design and characteristics of DRA to address the need of wireless communication systems.

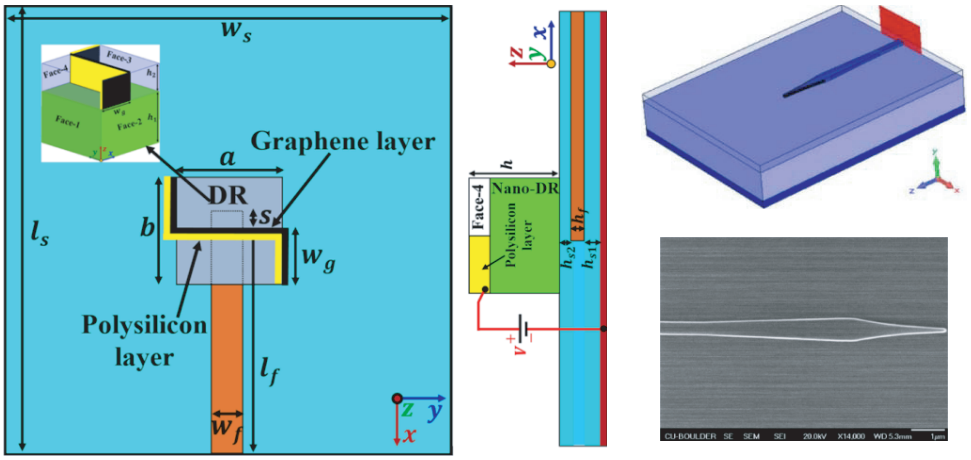

(a) (b)

Figure 1. (a) Simulated silicon-based NDRA geometry with side view [28], and (b) dielectric rod NDRA and image of the fabricated prototype of the antenna at optical frequencies [29].

2. THEORETICAL BACKGROUND

The prominent characteristic of DR radiations in open environment makes it suitable for antenna designing. DRA emerges as a new class in antenna designing that consists of the main radiating element formed of dielectric materials having relative permittivity ranges between 10 and 100. The aperture-coupled rectangular DRA with single-technique is shown in Fig. 2(a). The use of dielectric material as a radiator mitigates the conduction and surface wave losses in comparison to the conventional planar conducting antennas. The use of low loss tangent ($\tan\delta \leq 10^{-4}$) and high permittivity (ϵ_r) DR in bounded region allows to maintain high Q-factor. However, the radiating characteristic of DR allows the open boundaries to radiate energy. This results in the reduction of the Q-factor that provides wide bandwidth. DRA provides wide bandwidth, high gain, and improved radiation efficiency. One of the scintillating features of DRA offers the flexibility in shapes and aspect-ratio of the DR in order to achieve the desired characteristics of antenna [43, 44]. It provides additional degree of freedom in

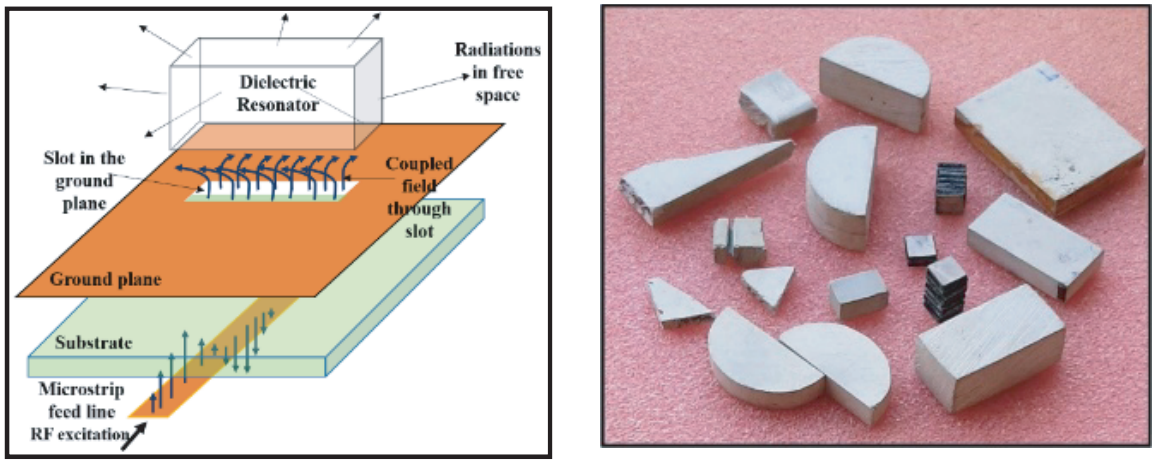

(a) (b)

Figure 2. (a) Aperture-coupled dielectric resonator antenna (DRA) and (b) different geometries of dielectric resonators.

dimension selection. Fig. 2(b) shows different shapes of the DRs like rectangular, triangular, cylindrical and stacked ones, etc.

Different shapes encompass the variations in the field distribution inside the DR that results in the existence of distinct mode configurations. This corresponds to different far-field characteristics and radiation efficiencies [27]. The DR parameters and position of the DR can be changed for the improvement in coupling and matching with the feeding mechanism. Consequently, operating bandwidth of the DRA can be changed over the wide range of frequencies by optimizing the dimensions of the radiator. The simple geometries and feeding schemes propound effective integration with other on-chips and networking communication systems. Hence, these features make DRA a suitable candidate in the antenna designing of microwave and millimeter-wave frequency applications.

Ritchmayer in 1939 investigated the evidence of radiations from DR experimentally [1]. The operating principle of DRA depends upon the concept of DR radiations in free space due to excitation. Ritchmayer considered the finite dimensions of DR surrounded by free medium placed inside the sphere having spherical coordinates (r, $\theta\phi$) and assigned the periodic solutions of Maxwell's equations. The fundamental set of solutions was considered for the field outside the region of sphere having radius, R, using the vector wave equation analysis in a spherical polar coordinates system. The power was assumed proportional to the sum of the squares of the absolute value of these coefficients for the fundamental set of solutions. The vanishing of these coefficients implies that there is no power radiation outside the sphere of radius, R. However, by the principle of analytical continuation for these solutions, there must be identical vanishing nature of the field in the open region or just outside the DR. Applying the boundary conditions, the tangential and normal components of electric field intensity, E, and displacement, D, must be continuous on the outer surface of the resonator. As dielectric constant is assumed to be finite, the field must vanish just at the outer region of the DR that concludes zero non-radiating field everywhere. The second-order wave equation is considered in time derivatives. However, the electromagnetic wave nature implies that the field cannot be zero outside the DR if oscillations exist. This depicts that field must lie outside the DR due to the motion of ions as the result of current distribution. Hence, oscillations outside the DR result in power radiations. This proves the phenomenon that DR radiates in free space. For the operating principle of DRA, there are mainly three categories of boundary conditions in different media explained as electric wall, magnetic wall, and dielectric-dielectric interface [45]. The Maxwell's equations in these media can be depicted as shown in Table 1.

In electric wall boundary condition, all the components must be zero inside the conducting medium.

Table 1. Boundary conditions in different media.

Conductor Interface (Electric Wall)	$\hat{n}\vec{D} = \rho_s$	(1a)
	$\hat{n}\vec{B} = 0$	(1b)
	$\hat{n} \times \vec{E} = 0$	(1c)
	$\hat{n} \times \vec{H} = J_s$	(1d)
Magnetic Interface (Magnetic Wall)	$\hat{n}\vec{D} = 0$	(2a)
	$\hat{n}\vec{B} = 0$	(2b)
	$\hat{n} \times \vec{E} = -\vec{M}_s$	(2c)
	$\hat{n} \times \vec{H} = 0$	(2d)
Dielectric Interface (Coupled Region)	$\hat{n}\vec{D}_1 = \hat{n}\vec{D}_2$	(3a)
	$\hat{n}\vec{B}_1 = \hat{n}\vec{B}_2$	(3b)
	$\hat{n} \times \vec{E}_1 = \hat{n} \times \vec{E}_2$	(3c)
	$\hat{n} \times \vec{H}_1 = \hat{n} \times \vec{H}_2$	(3d)

where $\vec{E}$ is the electric field intensity; $\vec{H}$ is the magnetic field intensity; ρ_s is the electric surface charge density; $\vec{D}$ is the electric flux density; $\vec{B}$ is the magnetic flux density; $\vec{M}$ and $\vec{J}$ are the magnetic and electric current densities, respectively.

Equations (1a)–(1d) explain the Maxwell's equations in the case of electric wall. These equations imply that the tangential component of $\vec{E}$ must be absorbed at the conducting surface. Similarly, the tangential component of $\vec{H}$ must vanish at the magnetic surface in the case of magnetic wall boundary condition as depicted in the Equations (2a)–(2d). However, in the case of dielectric-dielectric interface, both the components $\vec{E}$ and $\vec{H}$ remain continuous and behave as the coupled region condition as shown in Equations (3a)–(3d). Here in the case of DRA, the electric wall conditions are not applicable as the main radiator is made of dielectric material. The tangential component of $\vec{H}$ is the only source of energy between DR and free space. However, it becomes zero as per the magnetic boundary condition. Hence, the coupled region boundary condition can be applied to the DRA operation. When RF excitation is fed inside the DRA through feedline, the wave inside the DR starts bouncing back and forth within the dielectric walls and forms standing waves. These waves store energy in the form of oscillating $\vec{E}$ and $\vec{H}$ field components. Due to the accelerated and de-accelerated charged particles, the time-varying field starts radiating away from the DR in open space. The magnetic field starts to leak out from the transparent walls of the DR due to the fringing effect [46]. These fields in the form of electromagnetic waves radiate in open environment.

3. RESONANT MODES IN DRA

The current distribution inside the DR results in the specific field distribution at the resonant frequency. This periodic resonant frequency certainly acquires the maxima and minima depending upon the set of variables. The field distribution inside the resonator corresponds to the resonant mode [1]. This can be easily confirmed using the concept of Q-factor as the periodic function of frequency (ω). Because of the resonant mode inside the DR, the radiation characteristics can be predicted and analysed. These are broadly categorised into TE, TM and HEM modes which exist in DRA. Van Bladal has mainly classified the modes inside the arbitrary shaped DR as the confined and non-confined modes [6, 47]. Based on the boundary conditions, these modes can be defined using Equations (4a)–(4b).

$$\hat{n} \cdot \vec{E} = 0 \tag{4a}$$

$$\hat{n} \times \vec{H} = 0. \tag{4b}$$

Here, $\hat{n} = \frac{\vec{n}}{|n|}$ is the outward normal unit vector. $\vec{E}$ and $\vec{H}$ are the electric and magnetic field intensities, respectively.

According to these conditions, the modes that can follow both the conditions are considered as confined modes. However, the modes that can only satisfy the first condition are categorized as the non-confined modes [48]. The lowest order confined mode acts as an electric dipole. For instance, $TM_{01\delta}$ mode of cylindrical DR is the confined mode with the field pattern resembling the vertical electric monopole. However, the lowest order non-confined modes act as a magnetic dipole. The fundamental $TE_{11\delta}$ mode is the example of non-confined modes as the field pattern confirms the existence of horizontal magnetic dipole.

Figure 3 shows the E and H field distributions inside the electric and magnetic dipole. The short electric dipole can be analysed via an electric current carrying wire surrounded by magnetic field as

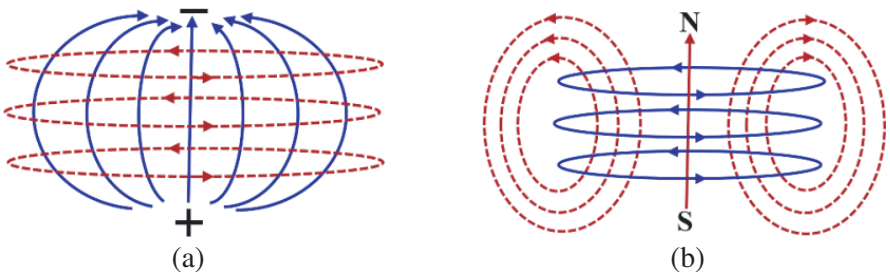

Figure 3. Field distribution in (a) short electric dipole and (b) short magnetic dipole (blue solid line-electric field and red dotted line-magnetic field).

shown in Fig. 3(a). In the same analogy, the short magnetic dipole can be considered as the electric loop that surrounds the magnetic flux lines shown in Fig. 3(b). It can be analysed that the radiations from the electric and magnetic dipoles are normal to its axis. The short electric and magnetic dipoles radiate in the boresight and end-fire direction, respectively. Hence, the co-polarized component of one of the dipoles becomes the cross-polarized component of the other.

3.1. Mode Analysis in Rectangular DRA

Van Bladel reported that the confined modes could only exists in the body of revolution like sphere and cylinder. However, rectangular dielectric bodies only support non-confined modes [47]. The TM modes in a rectangular DRA do not support the boundary condition explained in Equation (1) using DWM model. Thus, a rectangular DRA does not support the existence of TM_{mnp} modes, and only TE_{mnp} mode exists. The indices of the mode's nomenclature denote the field variations along the x, y, and z-axes, respectively. The field Equations (5a)–(5f) of the rectangular DRA can be evaluated using DWM model assuming the direction of propagation along z-direction as follows [31]:

$$E_x = k_y \left\{ \begin{array}{c} \cos(k_x x)\sin(k_y y) \\ \sin(k_x x)\sin(k_y y) \end{array} \right\} \cos(k_z z) \tag{5a}$$

$$E_y = -k_x \left\{ \begin{array}{c} \sin(k_x x)\cos(k_y y) \\ \cos(k_x x)\cos(k_y y) \end{array} \right\} \cos(k_z z) \tag{5b}$$

$$E_z = 0 \tag{5c}$$

$$H_x = \frac{(k_x k_z)}{j\omega\mu_o} \left\{ \begin{array}{c} \sin(k_x x)\cos(k_y y) \\ \cos(k_x x)\cos(k_y y) \end{array} \right\} \sin(k_z z) \tag{5d}$$

$$H_y = \frac{(k_y k_z)}{j\omega\mu_o} \left\{ \begin{array}{c} \cos(k_x x)\sin(k_y y) \\ \sin(k_x x)\sin(k_y y) \end{array} \right\} \sin(k_z z) \tag{5e}$$

$$H_Z = \frac{(k_x^2+k_y^2)}{j\omega\mu_o} \left\{ \begin{array}{c} \cos(k_x x)\cos(k_y y) \\ \sin(k_x x)\cos(k_y y) \end{array} \right\} \cos(k_z z) \tag{5f}$$

Table 2 shows the E-field distribution inside the rectangular DR for different mode configurations

Table 2. Mode analysis inside the rectangular DR [48].

Mode with field distribution	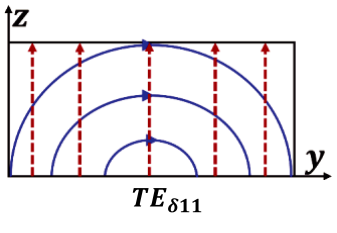 $TE_{\delta 11}$	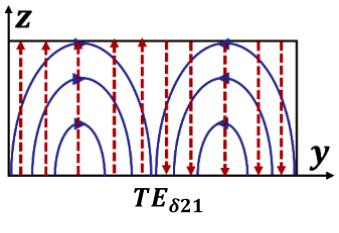 $TE_{\delta 21}$	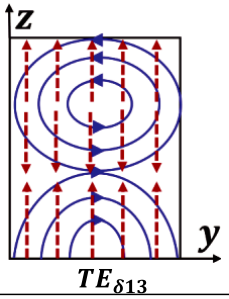 $TE_{\delta 13}$
Boundary condition	Magnetic wall	Magnetic wall	Electric wall
Dipole orientation	Transverse magnetic dipole	Transverse magnetic quadrupole	Transverse magnetic quadrupole
Field inside the DR	$E_z = 0$ $H_z = A\frac{(k_x^2 k_y^2)}{j\omega\mu_0}\cos(k_x x)\cos(k_y y)\cos(k_z z)$ where A is an arbitrary constant, and k_x, k_y and k_z denote the wavenumbers along the x-, y-, and z-axis, respectively.		

(Blue solid line: ***E*-field** and Red dotted line: ***H*-field**)

classified as TE_{mnp} [46]. The existence of TE modes inside the DR was experimentally verified in [49]. These modes confirm the presence of horizontal magnetic dipole.

3.2. Mode Analysis in Cylindrical DRA

The most basic and simple geometries of DR consist of cylinder and rectangular shapes. The cylindrical resonator allows the existence of TE_{mnp}, TM_{mnp}, and HEM_{mnp} modes. The indices of the mode nomenclature show the variations of the field along azimuthal (ϕ), radial (r), and height (z) axes, respectively, of the cylindrical DR. The fundamental dominant modes in cylindrical DRAs can be classified as $TE_{01\delta}$, $TM_{01\delta}$, and $HEM_{11\delta}$. Here, δ represents the incomplete axial variation considering z-axis as the direction of field propagation. The resonant frequencies of these dominant modes can be arranged as $TE_{01\delta} < TM_{01\delta} < HEM_{11\delta}$. The approximate field equations for the corresponding modes of the cylindrical DRA can be estimated as explained in [31, 50].

For $TE_{01\delta}$ mode of cylindrical DRA:

$$H_r \propto J_1(\beta r)\sin\left(\frac{\pi z}{2h}\right) \tag{6a}$$

$$H_\phi = 0 \tag{6b}$$

$$H_z \propto J_0(\beta r)\sin\left(\frac{\pi z}{2h}\right) \tag{6c}$$

$$E_r = 0 \tag{6d}$$

$$E_\phi \propto J_1(\beta r)\cos\left(\frac{\pi z}{2h}\right) \tag{6e}$$

$$E_z = 0 \tag{6f}$$

Here, $J_0(\beta r)$ and $J_1(\beta r)$ are the zeroth order and first-order of the first kind Bessel's functions, respectively. For $(r = a)$, radius of the cylindrical DR, β is the solution to $J_0(\beta a) = 0$. Similarly, for $TM_{01\delta}$ mode, the E- and H-field equations can be interchanged in Equations (6a)–(6f) for the approximate field analysis. Likewise, for $HEM_{11\delta}$ mode:

$$H_r \propto J_1(\alpha r)\cos\left(\frac{\pi z}{2h}\right)\left\{\begin{array}{c}\sin\phi\\ \cos\phi\end{array}\right\} \tag{7a}$$

$$H_\phi \propto \frac{\partial J_1(\alpha r)}{\partial(\alpha r)}\cos\left(\frac{\pi z}{2h}\right)\left\{\begin{array}{c}\cos\phi\\ \sin\phi\end{array}\right\} \tag{7b}$$

$$H_z = 0 \tag{7c}$$

$$E_r \propto \frac{\partial J_1(\alpha r)}{\partial(\alpha r)}\sin\left(\frac{\pi z}{2h}\right)\left\{\begin{array}{c}\cos\phi\\ \sin\phi\end{array}\right\} \tag{7d}$$

$$E_\phi \propto J_1(\alpha r)\sin\left(\frac{\pi z}{2h}\right)\left\{\begin{array}{c}\sin\phi\\ \cos\phi\end{array}\right\} \tag{7e}$$

$$E_z \propto J_1(\alpha r)\cos\left(\frac{\pi z}{2h}\right)\left\{\begin{array}{c}\cos\phi\\ \sin\phi\end{array}\right\} \tag{7f}$$

Here, for $(r = a)$, radius of the cylindrical DR, α is the solution to $J_0(\alpha a) = 0$.

Table 3 shows the field distribution of modes inside the cylindrical DR along with the features and field equations as reported in [27].

4. PERFORMANCE IMPROVEMENT TECHNIQUES IN DRA

The advancements in the field of DRA demands the generation of various techniques to improve the performance characteristics like impedance bandwidth, AR bandwidth, high gain, and improved radiation characteristics. Various review articles in the literature have explored the DRA for the enhancement of these parameters [27, 51–53]. The advancement in wireless communication system requires MIMO antenna systems. Various MIMO DRAs have been reported in the literature in the past decades [50]. Also, researchers are focussing on exploring the DRAs at millimetre-wave frequencies [54]. The detailed analysis of the techniques and improvements in DRAs is discussed as follows.

Table 3. Mode analysis inside the cylindrical DR [27].

Mode with field distribution	Boundary condition	Dipole orientation	Field inside the DR
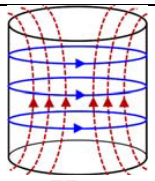 $TE_{01\delta}$	Magnetic wall	Axial magnetic dipole	$E_z = 0$ $H_z = J_o(hr)\cos\beta z$
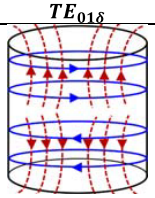 $TE_{011+\delta}$	Electric Wall	Axial magnetic quadrupole	$E_z = 0$ $H_z = J_o(hr)\sin\beta z$
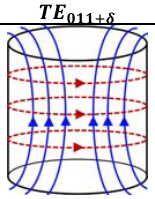 $TM_{01\delta}$	Electric Wall	Axial electric dipole	$E_z = J_o(hr)\sin\beta z$ $H_z = 0$
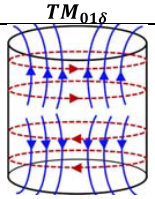 $TM_{011+\delta}$	Magnetic wall	Axial electric quadrupole	$E_z = J_o(hr)\cos\beta z$ $H_z = 0$
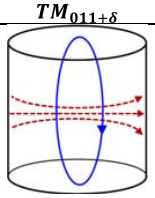 $HEM_{11\delta}$	Electric wall	Transverse magnetic dipole	$E_z = J_1(hr)\cos\beta z\begin{pmatrix}\cos\phi\\ \sin\phi)\end{pmatrix}$ $H_z \approx 0$
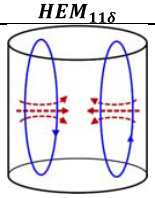 $HEM_{21\delta}$	Electric wall	Transverse magnetic quadrupole	$E_z = J_1(hr)\cos\beta z\begin{pmatrix}\cos(2\phi)\\ \sin(2\phi)\end{pmatrix}$ $H_z \approx 0$
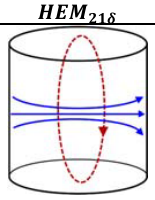 $HEM_{12\delta}$	Magnetic wall	Transverse electric dipole	$E_z \approx 0$ $H_z = J_1(hr)\cos\beta z\begin{pmatrix}\cos\phi\\ \sin\phi\end{pmatrix}$
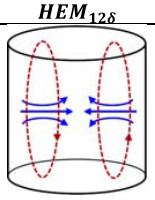 $HEM_{22\delta}$	Magnetic wall	Transverse electric quadrupole	$E_z \approx 0$ $H_z = J_2(hr)\cos\beta z\begin{pmatrix}\cos(2\phi)\\ \sin(2\phi)\end{pmatrix}$

4.1. Bandwidth Enhancement Techniques

Over the decades, DRAs have gained the focus of researchers due to the achievement of wide bandwidth in comparison to the other reported antennas. In this regard, several techniques and methods were reported to enhance the bandwidth of the antenna. Some of the techniques adopted for the achievement of bandwidth enhancement in DRAs are discussed in this article. The stacking of DRs technique generally includes the stacking of similar or differently shaped DR slabs having different dielectric permittivity materials. In 1989, Kishk et al. reported a broadband stacked DRA with 25% of reported bandwidth [14]. A concept of the air-gap insertion between the stacked driven and parasitic elements was reported for the bandwidth enhancement in an aperture-coupled cylindrical DRA [55]. A T-shaped stacked DRA was reported with coaxial probe feeding technique having more than 60% bandwidth [56]. Later, numerical and experimental investigation of a coaxial probed stacked DR was reported with the bandwidth enhancement technique [57]. A multi-layer structured DR of high permittivity material was reported with bandwidth improvement method [58]. The stacking of DRs affects the aspect-ratio of the antenna that leads to the generation of higher order modes inside the radiating element. The merging of higher order modes provides the bandwidth enhancement in DRA. An ultra-wideband DRA was reported with 148.6% bandwidth consisting of conical and cylindrical DRs stacking [59]. The wideband response was obtained due to the multiple resonance occurred in the hybrid structure of the DR. The antenna geometry, prototype, and bandwidth response of the reported antenna are shown in Fig. 4(a).

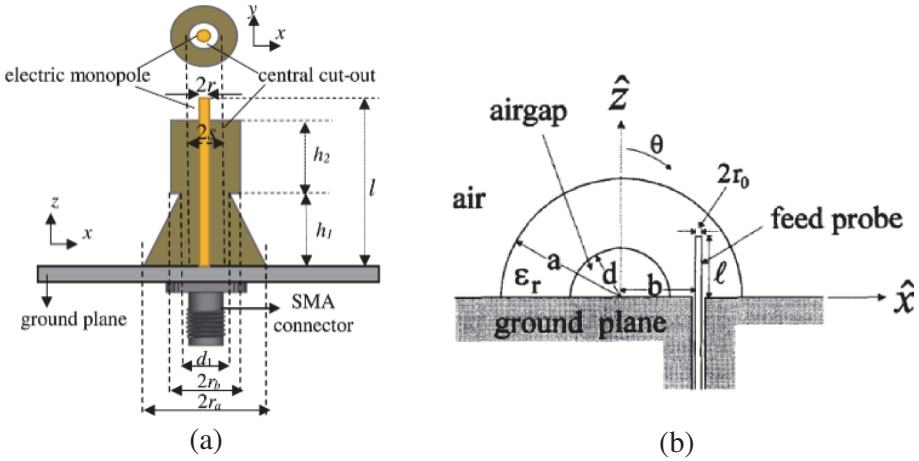

Figure 4. (a) Stacking of DR elements [59], (b) hemispherical DRA with air gap [60].

In the technique of crating the air-gap inside the DR, a portion of DR has been carved off from the DR to perturb the field distribution so that Q-factor of the DR is reduced to modify the radiation mechanism and enhance the bandwidth of the DRA. A hemispherical DRA with an air-gap between the dielectric material and ground plane is shown in Fig. 4(b). In this DRA, the effect of the air-gap was theoretically studied using the Green's function formulation [60]. A broadband DRA was reported with the introduction of an asymmetrical moat in the form of air-gap [61]. The perturbation in the E-field distribution results in the merging of adjacent modes TE^{y}_{111}, TE^{y}_{112}, and TE^{y}_{113} due to the reduction in Q-factor for bandwidth broadening. A rectangular DRA structure having an air-gap beneath the DR and shorted strip was reported with the 96% of impedance bandwidth [62]. The other techniques for obtaining bandwidth enhancement include placing a conducting patch at the top of the DR. Some of these techniques of the reported work are shown in Fig. 5. A hybrid DRA design was reported witha soft cylindrical surface in the form of metallic strip providing wide bandwidth [63]. However, the reported antenna requires extra feeding mechanism. In addition, a metamaterial superstrate can be used as a parasitic patch placed at some height from the DR to achieve the high directivity and enhancement in bandwidth [64, 65].

The half-split cylindrical DR was excited by hybrid $HEM_{11\delta}$ and $HEM_{12\delta}$ modes to enhance the impedance bandwidth of the antenna [67]. Moreover, the two-segments or multi-segmented DRA has

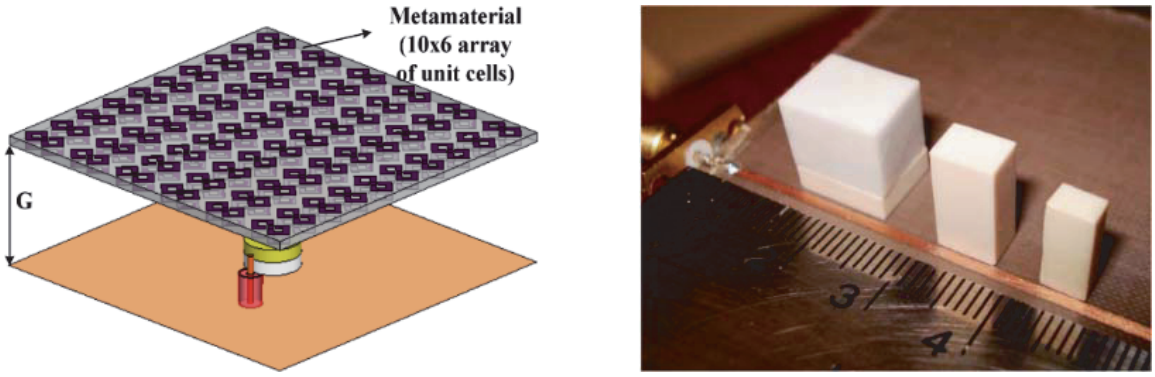

(a) (b)

Figure 5. (a) Cylindrical DRA with metamaterial-based superstrate [65] and (b) multi-segmented rectangular DRA [66].

been used with the low and high permittivity DR. In this inhomogeneous structure, it is supposed that the lower segment of high permittivity acts like an impedance transformer while the upper segment with low permittivity is the main segment that can be managed to obtain wide impedance bandwidth using low permittivity materials [66, 68]. However, the insertion of DR inside the other DR is a complex process and the limitation of such structures. Table 4 shows the detailed analysis of the reported bandwidth enhancement techniques in DRAs.

4.2. Gain Enhancement Techniques

There are various gain enhancement techniques reported in the literature in the field of DRA. The higher gain of the DRA is mainly related to the excitation of higher order modes inside the radiator. The stacking of DRs generally includes the stacking of the dielectric slabs of the materials having different relative permittivities. The increase in the height of DR due to stacking results in the merging of higher-order modes that enhances the gain of the antenna. Fakhte et al. reported an anisotropic cylindrical DRA with gain improvement [74]. The stacking technique in this reported work affects the overall aspect ratio (height to radius) of the antenna that increases the boresight gain of the antenna. The geometry and frequency response of the gain for this reported DRA are shown in Fig. 6(a).

Furthermore, they have also reported the rectangular DRA using uniaxial material and engraved grooves on the side walls of the stacked DRA for gain enhancement [76, 77]. However, these antennas have the limitation of increased height due to stacking. A double-layered DR of material having high

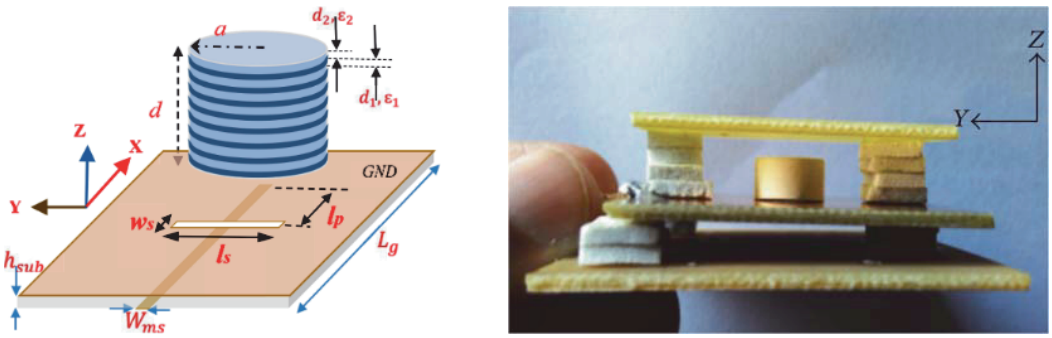

(a) (b)

Figure 6. (a) Stacked cylindrical DRA geometry [74], (b) fabricated prototype of the cylindrical DRA with reflector and superstrate [75].

Table 4. Reported DRAs with bandwidth enhancement techniques in the literature.

Techniques	**Summary**	**Advantages and limitations**	**Ref.**	**Bandwidth** (%)
Stacking	This technique generally includes the stacking of the dielectric slabs of the materials having different relative permittivity	The height of the DR remains same as in the isotropic DR.	[14, 55–59]	13.2, 10.49, 37, 60, 148.6, 25,
By loading of the conducting patch	Placing the conducting patch at the top of the DR enhances the bandwidth.	Needs extra feeding	[63, 69, 70]	27, 4.8, 22.1
Crating air gap inside the DR	A portion of DR has been carved off from the DR to perturb the field distribution so that Q factor of the DR reduced to modify the radiation mechanism and enhances the bandwidth of the DRA	Complex fabrication	[60, 62, 71, 72]	33, 96, 11.5, 24
Using Superstrate	A metamaterial superstrate is used as a parasitic patch placed at some height from the DR to achieve the directivity and enhancement in bandwidth.	Complex fabrication	[64, 65]	48, 22.19
Using half-split cylinder	The half split cylinder excited in the $HEM_{11\delta}$ and $HEM_{12\delta}$ modes enhance the impedance bandwidth of the antenna	Simple design configuration	[73]	35
Using multi-segment segmented DRA	The two segments of DRA have been used with the low and high permittivity DR. In this inhomogeneous structure, it is supposed that the lower segment of high permittivity acts like an impedance transformer while the upper segment with low permittivity is the main segment and can be managed to obtain wide impedance bandwidth using low permittivity materials	The insertion of DR inside the other DR is a complex process	[66, 68]	11.1, 68.1

permittivity was reported with 25% reduction in the overall size of a single-layered antenna [78]. This technique of using superstrate and reflector in DRA includes the use of superstrate above the DRA to increase the gain of the antenna. Various research works have been reported on the gain enhancement of the DRA using superstrates [79–81]. Superstrate is a parasitic patch placed at some height from the DR. This enhances the gain by confinement of the field before radiation. However, it increases the

overall size of the antenna. In addition, it requires some microwave material like foam between the DR and superstrate in the antenna hardware. In addition, the technique of using a reflector below the antenna structure provides more directive radiations from the antenna pointing the radiated power in the boresight direction. A cylindrical DRA with the approach of using the flat plane reflector was reported [82]. However, like superstrate, it also increases the size of the antenna due to the use of a reflector at the bottom in some distance from the ground plane, and the use of microwave material like foam causes some mechanical instability in the structure. An experimental study of utilizing both a superstrate and reflector in DRA has been reported in the literature for gain enhancement technique [75, 83]. Fig. 6(b) shows the prototype of the DRA with superstrate and reflector.

Further, the virtues of the electromagnetic bandgap (EBG) structures for gain enhancement of DRA have been utilized. EBG is an artificial material that exhibits unique electromagnetic properties, which are not achievable from the conventional materials. EBG materials are found to have stopbands where electromagnetic wave propagation is prohibited. This feature has attracted researchers to use EBG structures in antenna design to block surface-wave from propagating, and hence, to improve the radiation characteristics of the antenna. Several research works of using EBG structure with DRA have been reported in the literature [84, 86, 87]. However, these additional structures have the limitations of the increase in fabrication complexity with the DRA. Fig. 7(a) shows a DRA prototype of the antenna with EBG structures in one of the reported work. Other techniques include the loading of a conducting patch at the top of the DR surface to enhance the gain [88]. An effective technique of using horn cavity can also be used for the gain enhancement in DRA as shown in Fig. 7(b) reported in the literature. In this method, a DR is placed above the horn type cavity which leads to confining the field resulting in the enhancement of the gain [85]. Another technique includes increasing the height of the DR. This technique is somehow like the stacking of the dielectric slabs. But the only difference is that we use the dielectric materials of same permittivity. The concept behind the increment in height of the DR leads to the excitation of the higher order modes in the DR [89]. However, it adds on to the limitation of increased size of the antenna. Table 5 shows the detailed analysis of the reported gain enhancement techniques.

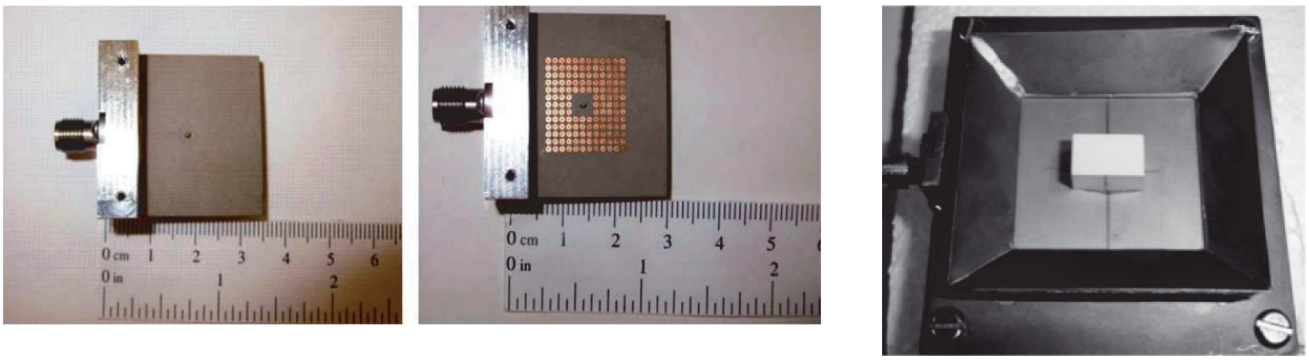

(a) (b)

Figure 7. (a) Fabricated prototype of the cylindrical DR with and without EBG structures [84], and (b) rectangular DRA place inside the horn cavity [85].

4.3. Circular Polarization Generation Techniques

To overcome the problem of antenna misalignment, multipath distortion and signal distortion, CP antennas are highly required. Over the past decades, CPDRAs have gained the attention of researchers. There are certain techniques that involve the generation of CP response in DRAs. The excitation of orthogonal degenerate modes results in the CP response. Some of the techniques reported in the literature include using specific feeding techniques, modified shape of the slot, modified geometry of the DR, and many more for the AR bandwidth enhancement. Single/multi-feeding mechanism utilizes the specific feeding mechanism in the antenna design that incorporates the generation of orthogonal

Table 5. Reported DRAs with gain enhancement techniques in the literature.

Technique	Summary	Advantages and limitations	Ref.	Gain (dBi)
Stacking	This technique generally includes the stacking of the dielectric slabs of the materials having different relative permittivity's	The height of the DR remains same as in the isotropic DR.	[74, 77, 78, 90–92]	5–1
Increasing the height of the DR	This technique is somehow like the stacking of the dielectric slabs. But the only difference is here we use the dielectric materials of same permittivity. (In this case the higher order modes are excited in the DR by increasing the height)	The height of the DR needs to be increased for the enhancement of the gain of the antenna.	[89]	Up to 10
By loading of the conducting patch	Placing the conducting patch at the top of the DR enhances the gain.	Needs extra feeding	[93]	Up to 10
Using superstrate	Superstrate is the parasitic patch placed at some height from the DR. This enhances the gain by confinement of the field before radiation.	Large antenna size. In addition, it requires some microwave material like foam at between the DR and superstrate in the antenna hardware.	[75, 79–81, 83]	6–21
Using electromagnetic band gap structures	The EBG structures are artificial materials that exhibit unique electromagnetic properties, which are not achievable from conventional materials. EBG materials are found to have stopbands where electromagnetic wave propagation is prohibited. This feature has attracted the researchers to use EBG structures in antenna design to block surface-wave from propagating, and hence, to improve the radiation characteristics of the antenna.	Complex fabrication	[84, 86, 87]	6–11
Using reflector	Reflector is placed below the antenna structure. This provides the more directive radiations from the antenna pointing the radiated power in the boresight direction.	Large antenna size due to use of reflector at the bottom at some distance from the ground plane. It requires the microwave material like foam causing some mechanical instability.	[82]	6–11
Using horn cavity	In this technique, DR is placed above the horn type cavity which leads to confine the field resulting in the enhancement of the gain.	Large antenna size and complex hardware.	[85]	6–10

degenerate modes in the DR structure. A singly fed aperture-coupled rectangular DRA was reported in the literature with CP response [94]. This reported DRA consists of a DR rotated at 45° with respect to the aperture as shown in Fig. 11(a). Along with this, the aspect ratio of the antenna also plays the main role in CP generation, and it must satisfy the following quadrature phase condition given in Equation (8):

$$\frac{f_1}{Q_1} + \frac{f_2}{Q_2} = f_2 - f_1 \tag{8}$$

where f_1 and f_2 are the resonant frequencies. Q_1 and Q_2 are the unloaded Q-factors of the two modes.

In [95], the position of the coaxial feed in a circular sector DRA resulted in the excitation of $TM_{11\delta}$ and $TM_{21\delta}$ horizontally and vertically polarized modes. The generation of such modes provides the CP response of the antenna. The reported geometry of the CPDRA is shown in Fig. 8(a).

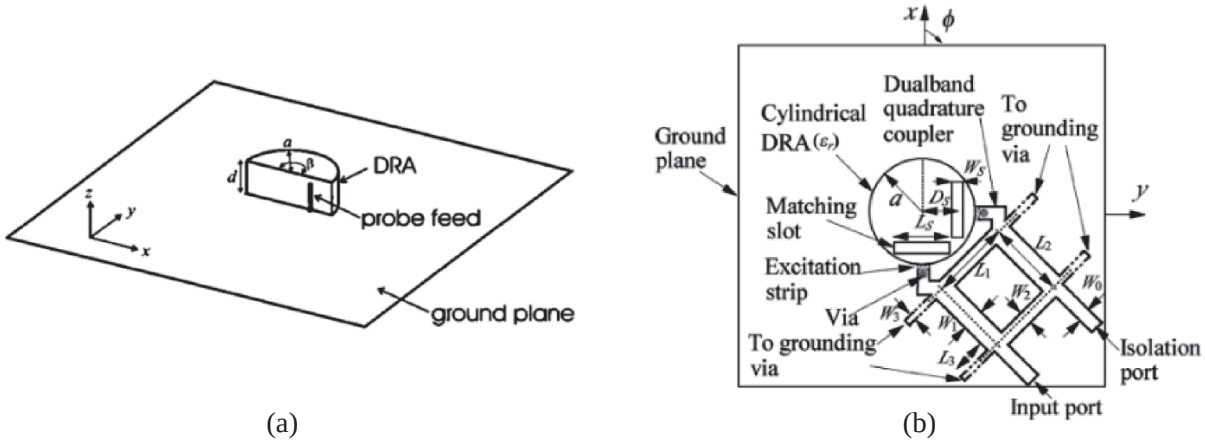

Figure 8. (a) Single-feeding techniques reported in literature as probe-fed half cylindrical CPDRA [95], and (b) CPDRA reported with quadrature strip feeding technique [96].

Another technique for CP generation utilizes the multi-feeding mechanism that results in the excitation of orthogonal degenerate modes. A CPDRA with quadrature strip-feeding technique has been reported with the generation of dual modes as shown in Fig. 8(b). This corresponds to the excitation of $HEM^x_{11\delta}$, $HEM^y_{11\delta}$, HEM^x_{113}, and HEM^y_{113} orthogonal degenerate modes in the lower and upper band, respectively for obtaining CP response [96]. A rectangular CPDRA with underlaid hybrid coupled was investigated to provide feeding at the four walls of the DR via metallic strip [97]. This results in the generation of four-quadrature signal that resulted in the wideband CP response. This reported antenna provides 27.7% of AR bandwidth. Similarly, a compact hollow CPDRA has been reported with the underlaid quadrature coupling technique [98]. However, this antenna required an external 50 Ω load for impedance matching that increases the complexity of the design. These techniques provide the wideband CP response. However, the main disadvantage of using multi-feeding techniques for CP generation is that it increases the structural complexity of the antenna.

Furthermore, the technique of using the specific shapes of the slot that generates the orthogonal degenerate modes inside the DR. This results in the achievement of the circularly polarized response of the antenna. Fig. 9(a) shows the modified crossed shape of the slot reported in the literature. A dual-band CPDRA with cross-slot was reported with the excitation of TE_{111} and TE_{121} orthogonal modes in the lower band and TE^x_{131} and TE^y_{131} orthogonal nearly degenerate mode in the upper band [99]. Later, different modified shapes were explored to obtain the CP response of the antenna including modified cross-slot [100, 101] and Archimedean spiral slot [102]. A wideband CPDRA has been reported with the stair-shaped slot excitation [103]. This antenna provided the 41.01% of the AR bandwidth with the excitation of TE_{111}, TE_{121}, and TE_{131} orthogonal degenerate modes inside the DR. The merging of these fundamental and higher-order modes resulted in the achievement of the wideband response of the antenna. With a similar concept, a rectangular CPDRA has been reported in the literature [104].

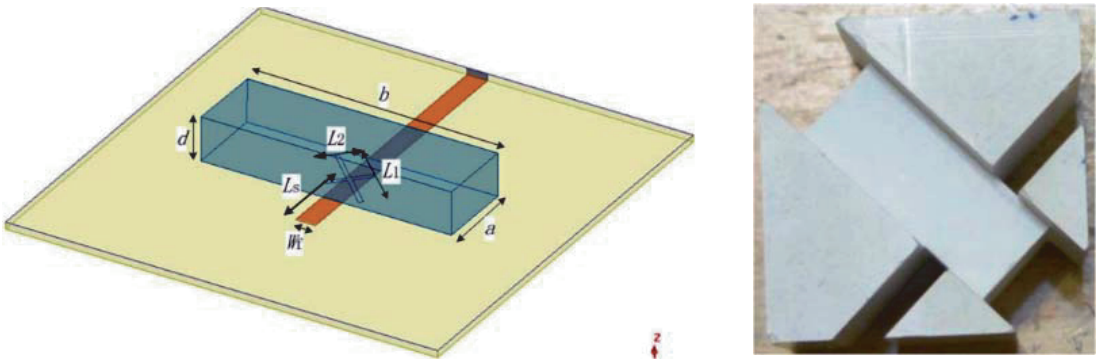

(a) (b)

Figure 9. (a) CPDRA reported with cross-slot [99], and (b) DR with diagonal slits [105].

In addition, different geometries of the DR have been reported in the literature as the CP generation technique. The specific modifications in the DR result in the generation of orthogonal degenerate modes. One of the reported structures is shown in Fig. 9(b). A CPDRA was reported with inclined slits to the sidewalls and diagonal of the DR [105]. This specific structure of the DR excited the degeneracy modes resulting in CP response of the DRA. A rectangular DR stacking with rotation angle between the elements was reported with the CP response [106]. Similarly, a rotated-stair rectangular DR has been reported with the proximity coupled feeding mechanism [107]. It provided 18.2% of AR bandwidth with TE_{111} and TE_{113} mode excitation for obtaining CP response. A wideband CPDRA had 43% of the AR bandwidth [108]. In this reported antenna, the geometry consists of unequal inclined slits in a rectangular DR with tapered metallic strips on the orthogonal walls resulting in the generation of the orthogonal degenerate modes. Specific arc-shaped and modified stair-shaped DR elements have been reported with CP response [109, 110].

The conducting strip consisted of copper material on the surface of the DR. The use of parasitic strip on the DR walls confines the orthogonal degenerate modes resulting in the achievement of CP response. There are several works reported on the use of strips for AR bandwidth enhancement. Some of the DR geometries with parasitic strip on the surface are shown in Fig. 10. A cylindrical CPDRA was reported with the use of parasitic strip, and its effect on the AR bandwidth has been investigated [111]. Also, It was studied that the change in the location of the metallic strip can tune the AR response in inverted-sigmoid DR [112]. An omnidirectional perturbed rectangular DRA was reported with the metallic strip on the diagonal slit of the DR providing the CP mode excitement [113]. A rectangular DR with conductive coating at the notches has been reported with the 55.22% of the AR bandwidth [114]. A

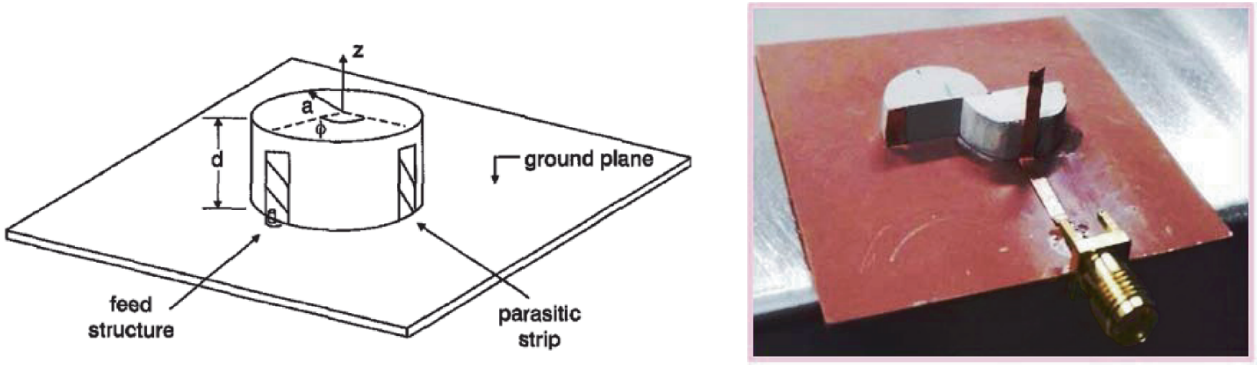

(a) (b)

Figure 10. The use of metallic strip on (a) cylindrical DR [111], and (b) inverted-sigmoid DR [112].

Table 6. State of art of the reported CPDRAs.

S. No.	f_c (GHz)	ϵ_r	Excitation	ARBW (%)	BW_{Im} (%)	Gain (dBic)
[116]	10	10	Probe	5.71	29.14	4.71–4.78
[107]	5.8	9.8	Hybrid slot	18.2	31	4.5
[117]	10	10.2	Aperture	6	21	6–6.7
[105]	5.2	10	Probe	210 MHz	130 MHz	NR
[118]	5.6	10.2	Side strip	22	37	5.7
[100]	2.6	11	Hybrid slot	24.6	28.6	5
[113]	3.6	15	Probe	25	24.5	2
[119]	2.4	15	Probe	7.3	24.4	2
[120]	2.4	9.4	Strip feed	12.4	32.5	6.44
[121]	4.2	9.3	Square spiral strip	14	11	4–5
[122]	3.2	9.2	Probe	13	20	NR
[123]	2.13	12	Spiral slot	25.5	NR	4.52
[106]	3.6	9.4	Rotated slot	21.5	33.5	5.28–8.40
[124]	10	12	Aperture	10.6	36.6	NR
[103]	4.7	12.8	Stair-shaped slot	41.01	49.67	> 1.5
[114]	4.7	12.8	Stair-shaped slot	55.22	69.11	2.06
[98]	2.42	10	Dual-feeding	33.8	24.95	6
[125]	2.6	10	Hybrid coupler	27.7	37	NR

f_c = centre frequency, ϵ_r = permittivity of the DR, **ARBW** = axial-ratio bandwidth, BW_{Im} = impedance bandwidth, and NR: not reported.

dual-band CPDRA with the metallic strip coating on the outer walls of the rectangular DR for obtaining circular polarization has been reported with miniaturization and frequency-ratio tuning concept [115]. Table 6 shows the reported circular polarization generation techniques developed over the years.

4.4. Miniaturization Techniques

The current research issue of DRA requires the development of miniaturization techniques. It provides the scope for the integration of DRA with the future technology. One of the commonly used techniques is the use of metallic or parasitic strips on the surface of DRs [115, 126–128]. However, the use of

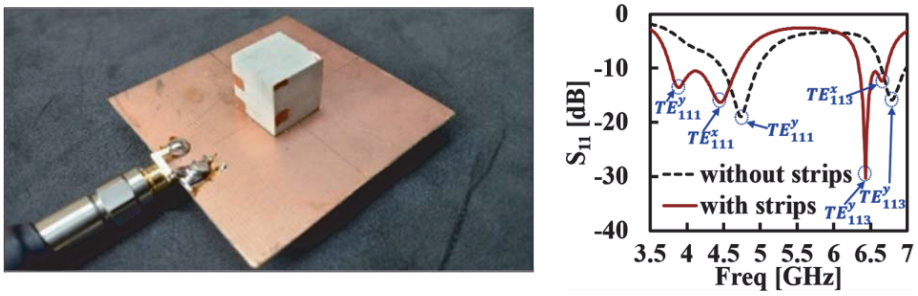

(a) (b)

Figure 11. (a) Fabricated prototype of the antenna using metallic strips, and (b) miniaturized dual-band response of the antenna [115].

metallic strips on the larger surface area reduces the radiation characteristic of the antenna [127]. A top loaded parasitic strip element DRA was reported with the dual-band operation [129]. Fig. 11(a) shows the fabricated prototype of the rectangular DRA with metallic strips on the outer surface for the achievement of miniaturization. In Fig. 11(b), the frequency response of the S_{11} parameter clearly shows the shifting of the operating frequency passbands to the lower frequency ranges using the metallic strips in this reported work [115]. Thus, miniaturization has been obtained. The other techniques include the use of high permittivity DR [130] and high aspect ratio DR [66]. A transparent metallo-DRA has been reported having integration with the amorphous silicon solar cells [131]. However, the method of using the high permittivity DR reduces the overall bandwidth of the antenna. Thus, apart from these studies, this field still requires a lot of developments for obtaining the miniaturization.

5. PERFORMANCE IMPROVEMENT IN MULTI-INPUT-MULTI-OUTPUT (MIMO) DRA

MIMO DRAs are single radiator [134, 135] and multi-radiator [136] antenna structures. The main limitation of a MIMO DRA with multi-radiators is that it compromises with the increased size of the antenna. On the other hand, the single radiator DRA enhances the compactness of the antenna. However, it becomes a very challenging task to maintain the isolation in the MIMO DRA with single radiator. In order to improve the isolation between the radiating elements, several wideband MIMO DRAs have been reported with parallel [137, 138] and orthogonal [132, 133] feeding mechanisms. The structures and prototype of the reported MIMO DRAs are shown in Fig. 12. Using the specific shapes and feeding mechanism in MIMO DRAs provides the wideband antenna response. An ultra-wideband two-port MIMO DRA with rectangular radiators and parallel feeding mechanism have been reported with 106% impedance bandwidth [139]. A super-wideband two-port MIMO DRA has been reported with 132.69% of operation bandwidth [140]. In this antenna, the specific inverted frustum shaped DR elements allow the merging of several higher-order modes resulting in the wideband response of the antenna. For the MIMO configuration in antennas, several diversity performance matrices are required to be in good agreement. These performance parameters include envelope correlation coefficient (ECC), total active reflection coefficient (TARC), diversity gain (DG), mean effective gain (MEG), and channel capacity loss (CCL) [141].

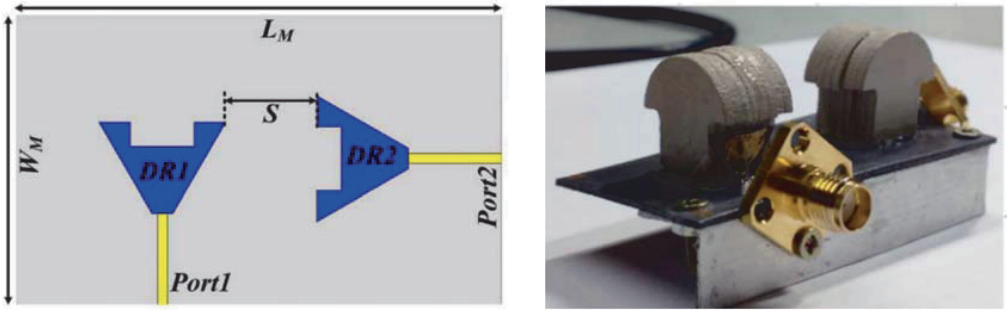

(a) (b)

Figure 12. Wideband MIMO DRAs with (a) A-shaped DR [132], and (b) mushroom-shaped DR [133].

Further, over the past decade, there are several techniques for obtaining the circular polarization in MIMO DRAs. These techniques mainly involve the use of the specifically shaped DR, metallic strips on the surface of DR, specific shape of the slots, and orthogonal feeding mechanism to excite the orthogonal degenerate modes for the achievement of CP response.

A two-port MIMO CPDRA with rectangular DRs have been reported with the modified cross-slots for the generation of CP modes [142]. Apart from this, to improve the isolation in this compact structure, a metallic strip has been utilized to decouple the electric field between the DRs. Another technique includes placing DRs diagonally to reduce the mutual coupling between the radiators as reported in [143]. This MIMO CPDRA uses parasitic strips at the specific location near the feeding to generate the CP

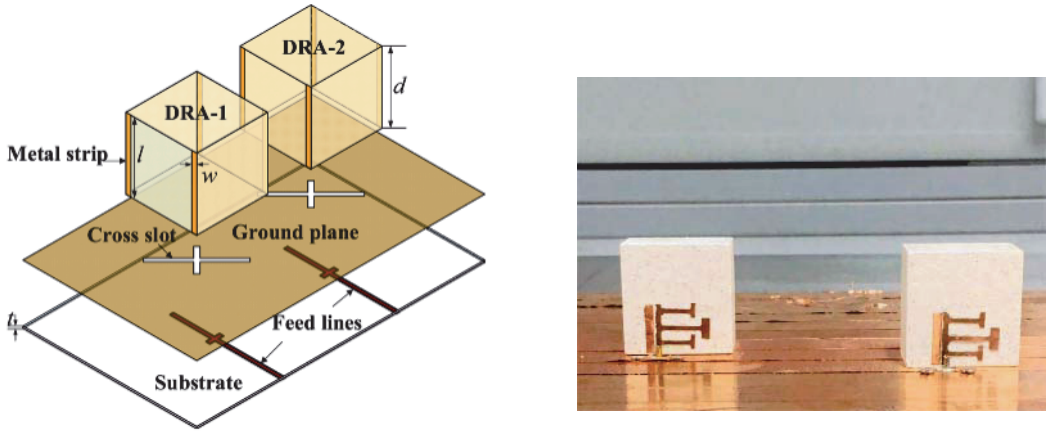

Figure 13. Circularly polarized MIMO DRAs with (a) rectangular DRs with metallic strips [142], and (b) diagonally placed DR with parasitic strips [143].

response. A technique utilizes different shapes including P-shaped [144], L-shaped [145], and modified rectangular-shaped DRs [146] for generating CP response in MIMO DRAs along with proper mutual coupling reduction techniques. Some of the reported DRAs are shown in Fig. 13.

Currently, researchers are constantly working for obtaining the diversity performance of the antenna. MIMO DRAs provide the diversity in the performance of the antenna. There are several MIMO antennas reported with polarisation and pattern diversity in the literature. Some of the reported designs and prototypes are shown in Fig. 14. A cross-shaped MIMO DRA has been reported with the polarization diversity providing CP and LP radiations using different ports [147]. The effects of the symmetric and asymmetric feeding mechanisms on the isolation between DR elements have been analysed.

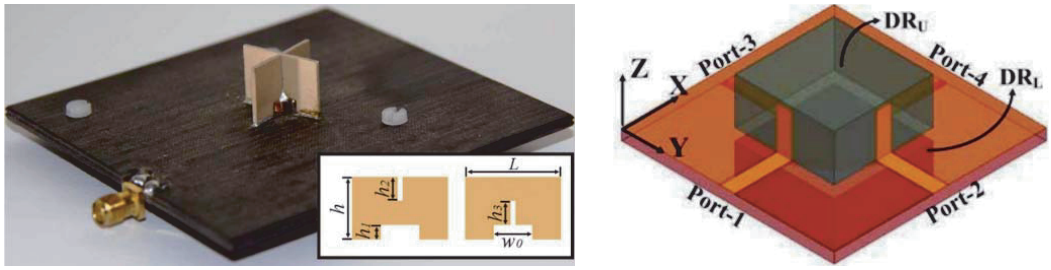

Figure 14. The reported (a) two-port cross-shaped [147] for polarization diversity, and (b) four-port double-sided rectangular DR [148] for pattern diversity.

This antenna had broadside CP and omnidirectional radiation pattern. The maintenance of isolation between the DR elements plays a crucial role in MIMO antenna designs. A two-port cylindrical DR has been reported with a modified circular slot that provides the dual sensing with LHCP and RHCP polarizations using different ports [149]. In this reported antenna design, the mutual coupling between the DRs has been reduced using defected ground structures (DGSs).

For pattern diversity, a four-port double-sided rectangular MIMO DRA with a coplanar waveguide using conformal patch feeding technique has been reported [148]. In this reported work, the excitation of the DR at different sides of the substrate resulted in the pattern diversity. In addition, the excitation of the orthogonal modes in DRA reduces the coupling between the DR elements. Recently, a compact four-port MIMO DRA has been reported with pattern diversity using two epsilon shaped and cylindrical

DRs separately fed using the conformal strip and coaxial probe feeding technique, respectively [150]. Apart from this, several other techniques including the use of frequency selective surface (FSS) [151], a three-port MIMO DRA with decoupled modes [152], and a six-port DRA array with MIMO analysis [153] have been reported in the literature for obtaining pattern diversity. Table 5 shows the detailed analysis of the reported MIMO DRAs in the literature. Table 7 shows the reported MIMO DRAs with analysis of detailed results.

Table 7. State of art of the MIMO DRAs with wide band response and CP response.

Wideband MIMO DRAs								
Ref.	**DR**	**Frequency range (GHz)**		**BW_{Im} (%)**		**Isolation (dB)**	**Peak Gain (dBi)**	
		P_1	**P_2**	**P_1**	**P_2**		**P_1**	**P_2**
[132]	A-shaped	3.24–5.98	3.24–6	59.2	60.9	20	6.03–7.45	
[154]	Mushroom shaped	5.08–9.50	4.89–9.61	61	65	20	3.34–7.4	2.34–7.9
[137]	Tree Shaped	3.95–10.4		89.9		17	-	
[139]	Rectangular	3.29–10.74		106		15	5.3	
[138]	Ring shaped	3.4–8.2	3.3–8.2	82.75	85.21	20	3	

Circularly polarized MIMO DRAs										
Ref.	**DR Shape**	**Number of DR Elements**	**Spacing between the DR elements**	**f_r (GHz)**	**f_{CP} (GHz)**	**BW_{AR} (%)**	**BW_{Im} (%)**		**Isolation (dB)**	**Gain (dBi)**
							P_1	**P_2**		**P_1** **P_2**
[149]	Cylindri-cal	Two	$\lambda/4$	5.75	5.75	3.50	15.1	14.9	23	4.7
[145]	L	Two	$\lambda/3$	5.5	5.4	4.60	17.16		15	3.8

f_r — resonant frequency of fundamental mode, f_{CP} — centre frequency at which CP is achieved, BW_{AR} — 3-dB AR bandwidth, BW_{Im} — 10-dB impedance bandwidth, P_1 — port-1 and P_2 — port-2 (in the case of CP antenna the unit of gain is dBic).

6. PERFORMANCE ANALYSIS OF NANO-DRAS AT THZ FREQUENCIES

The scintillating properties of DRAs like low conduction losses, high permittivity, and improved efficiency make them suitable for the niche developments in the microwave to optical frequency ranges of the electromagnetic spectrum. These features pave the path for efficient devices integration and on-chip applications at higher frequency ranges where the performance of metallic resonators degrades. It has been predicted that passive THz DRAs can be designed with the achievement of nearly 100% efficiency numerically for the applications like reflect array as investigated by the dispersive conductor model [41]. A magnetic mirror realised DRA using artificial magnetic conductor (AMC) has been demonstrated at 0.8 THz resonant frequency [155]. In this reported work, the fundamental magnetic dipole resonance of the cylindrical silicon wafer-based DRA was experimentally analysed. This was reported with the magnetic mirror operation having 30% of the operational bandwidth and about 97% of the radiation efficiency. The reported DR structure and fabricated prototype images are shown in Fig. 15. Table 8 shows the state of art of the reported nano-DRAs at THz regime. The advancements in wireless communication systems demand a high bandwidth and higher data rate that shifts the applications at THz frequency ranges. A rectangular DRA has been excited via a graphene-based plasmonic dipole at 2.4 THz frequency range [156]. This antenna supports the TE^{y}_{112} mode with radiation efficiency up to 70%. The graphene material has been widely used and considered as the perfect replacement of the metals due to poor electronic properties at THz frequencies. A silicon-based DR has been reported with the graphene disk on top layer responsible for the tuning of the impedance band of the antenna [157].

Table 8. State of art of the nano-DRAs at THz regime.

Ref.	Antenna structure	Operating frequency range (THz)	Resonant frequency (THz)	10-dB Impedance bandwidth (%)	Radiation efficiency (%)
[35]	Hexagon DR	190.9–198.1	193.5	3.7	NR
[158]	Folded silver dipole	NR	262	NR	18.8–37
[159]	Nano-dipole	345–355	350	2.85	20
[29]	Dielectric rod antenna	172–222	190	25.38	40–60
[160]	Triangular DR	192.5–197.3	193.5	2.58	NR
[161]	Cylindrical DR	185–205	193.5	10.25	NR

NR: *not reported.*

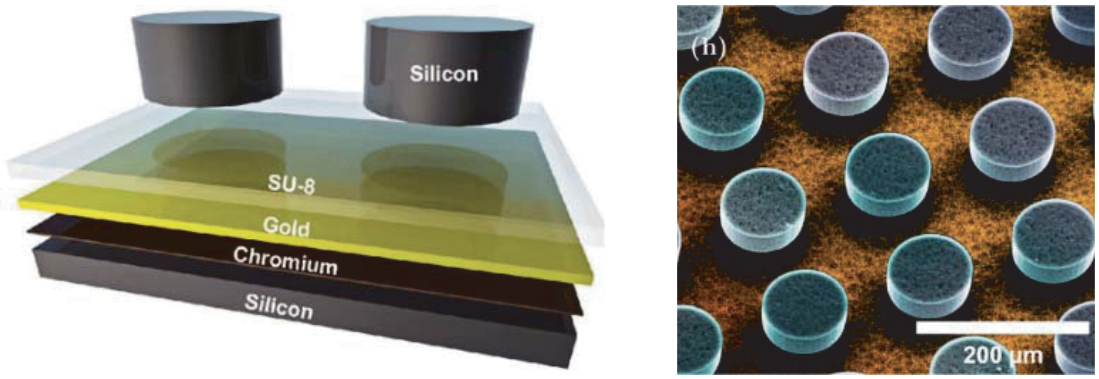

(a) (b)

Figure 15. (a) Artificial magnetic conductor (AMC) based DRA, and (b) false colour SEM image of the fabricated prototype [155].

This antenna excites the higher-order $HEM_{41\delta}$ mode inside the cylindrical disk DR. Recently, a silicon-based CPDRA has been reported with the graphene coating on the surface of the DR in specific fashion resulting in CP response at THz frequency range [28]. However, the dispersive properties of the metal conductivity lead to the plasmonic behaviour resulting in the dissipation losses at the optical frequencies.

Considering this, DRAs can substantially mitigate these losses. The availability of high-efficiency resonant elements is highly required in the optical domain. This can be efficiently realized for the future application that requires the manipulation of high-resolution light [162]. In the past few decades, the optical nano-antennas have also gained the attention due to several on-chip optical applications. The utilization of DRA and its concepts at optical frequencies has been widely explored for the futuristic technologies [163]. There are several differently shaped DRs including cylindrical [40], hexagonal [35], triangular [160] ones reported in the optical frequency regime. A dielectric rod NDRA was reported for the on-chip networking applications at the optical frequency band [29]. This reported work consists of multiple antennas at the optical signal hubs for on-chip networking. However, at nanoscale, tuning of the antenna orientation as per the required direction is a quite challenging task. CP nano-antennas can overcome this limitation. Recently, CP NDRAs have been reported with the circular polarization generation technique [34, 164]. The CP response has been obtained using the application of the Gaussian pulse excitation at the corner of the nanostrip feedline having quarter-wavelength path difference. This specific feeding mechanism splits the field into the orthogonal components across the edges of the

feedline. This fed the orthogonal degenerate modes inside the DR resulting in the achievement of the CP response. In applications like optical scanning microscopy, molecular sensing, optical magnetic recording wireless interconnects, and integrated circuits, CP nano-antennas can be employed as the source of circular polarization [165]. The left-hand CP (LHCP) and right-hand CP (RHCP) waves can be efficiently utilized for magnetization reversal. Hence, the achievement of CP response at THz and optical frequencies is quite advantageous for various nano-antenna based applications.

7. EXPLORING POSSIBILITIES OF DRAS WITH OTHER TECHNOLOGIES

With the advancements, DRA can efficiently provide the solutions for the system-in package technology. It provides the compact and better front-end subsystems modules than the other conventional approaches. In this era of modern communication systems, the combination of using filter before the radiating antenna is of great advantage to suppress the unwanted signals. In the RF front-end subsystems, filtenna shows the required deviation from the conventional approach of designing the components separately [166]. This maintains the compactness of the system. For this, DRA comes up as an efficient solution. Various compact filtenna systems with DRA integration have been reported in the literature [167–170]. In [171], a substrate integrated waveguide (SIW) filtering structure was reported with a DRA in order to enhance the bandwidth and suppressing the undesired harmonic resonances. Currently, RF and microwave sensors have been widely used for chemical sensing and material characterization [172]. Another possibility of DRA as sensors has gained the interest of the researchers. The permittivity of the DR is one of the crucial parameters, which affects the operating passband of the antenna to a great extent [173]. Thus, DRA responds with different resonant frequencies while working with different materials and chemicals. This approach is cost-effective with low power consumption and easy fabrication technique in comparison to the other conventional approaches. A cylindrical DRA sensor has been reported for the experimental validation of different chemical liquids [174].

In addition, the excitation of multiple modes inside the DR provides detailed analysis of the radiation mechanism of the antenna [129]. This can be widely used for various applications including biomedical devices [175]. The super wideband response is obtained due to the generation of higher order modes that provides the wider bandwidth due to the merging of modes [140]. Apart from this, the wide scope of the DRA reconfigurable antennas is reported in various research works. With the advancements, the concept of reconfigurability has gained the popularity nowadays [37]. These antennas provide the switchable pattern and polarization characteristics of the antenna using different excitation ports, modifications in the feeding networks, and PIN diodes [176]. Thus, there is a wide scope and possibilities of DRA with the other technologies. Fig. 16 shows the schematic chart representing the possibilities of DRA with other technologies.

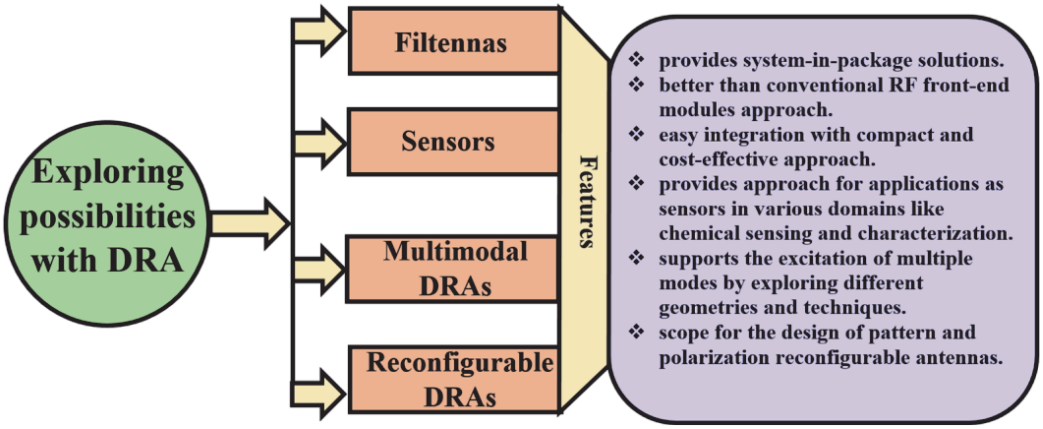

Figure 16. Schematic chart representing the possibilities of DRA with other technologies.

8. CONCLUSION

The critical analysis of the recent advancements and trends in the field of DRA have been presented in this paper. This study deals with the detailed analysis of the state of art of the exploration of the modes inside DRA and the various performance improvement techniques. These performance improvement techniques include the comprehensive analysis of the bandwidth enhancement, gain enhancement, and CP generation methods reported in the literature. With the advancements, higher data transfer rate is the prominent requirements for a communication system. This includes the increase in the channel capacity without exploiting the limited constraints like signal power and bandwidth. This needs the development in the field of MIMO antenna designs. Thus, the concept of MIMO in DRA is explored along with the diversity performance features. These features include the study of various performance matrices like envelope correlation coefficient (ECC), total active reflection coefficient (TARC), diversity gain (DG), mean effective gain (MEG), and channel capacity loss (CCL). Currently, researchers are working in the field of isolation improvement techniques, obtaining CP response, obtaining pattern and polarization diversity in MIMO DRAs. All these studies reported in the literature are limited to the microwave and sub-millimetre wave ranges. However, the THz and optical frequency regime remains to be explored in antenna designing. For this, the electronic features of the main radiating element play a very crucial role. Considering this, to mitigate the conduction losses at THz and optical frequencies, high-efficiency DRA proves rationale in extending towards the higher frequency ranges. These features define the scope for the efficient system integration and on-chip applications at higher frequency ranges where the performance of metallic resonators degrades. Another aspect of the possibility of nano-DRA fabrication has also been mentioned in this study. The achievement of CP response at THz and optical frequencies is quite advantageous for various nano-antenna based applications. These features of DRA can be efficiently realized for the future application that requires the manipulation of high-resolution light. Moreover, the possibilitoes of DRA in other technological fields like filtenna for RF front-end subsystems and sensors for chemical sensing have been addressed. Apart from this, the approach of utilizing the multiple modes of DRA and reconfigurability has been discussed. Thus, this study shows the concluding prominence of dielectric resonator antennas in the field of antenna designing and its futuristic approaches.

REFERENCES

1. Richtmyer, R. D., "Dielectric resonators," *J. Appl. Phys.*, Vol. 10, No. 6, 391–398, 1939.
2. Okaya, A. and L. F. Barash, "The dielectric microwave resonator*," *Proc. IRE*, Vol. 50, No. 10, 2081–2092, 1962.
3. Cohn, S. B., "Microwave bandpass filters containing high-Q dielectric resonators," *IEEE Trans. Microw. Theory Tech.*, Vol. 16, No. 4, 218–227, 1968.
4. Sager, O. and F. Tisi, "On eigenmodes and forced resonance-modes of dielectric spheres," *Proc. IEEE*, Vol. 56, No. 9, 1593–1594, 1968.
5. Van Bladel, J., "On the resonances of a dielectric resonator of very high permittivity," *IEEE Trans. Microw. Theory Tech.*, Vol. 23, No. 2, 199–208, 1975.
6. Van Bladel, J., "The excitation of dielectric resonators of very high permittivity," *IEEE Trans. Microw. Theory Tech.*, Vol. 23, No. 2, 208–217, 1975.
7. Kobayashi, Y. and S. Tanaka, "Resonant modes of a dielectric rod resonator short circuited at both ends by parallel conducting plates," *IEEE Trans. Microw. Theory Tech.*, Vol. 28, No. 10, 1077–1085, 1980.
8. Long, S. A. and M. W. McAllister, "The resonant cylindrical dielectric cavity antenna," *IEEE Trans. Antennas Propag.*, Vol. 31, No. 3, 406–412, 1983.
9. McAllister, M. W., S. A. Long, and G. L. Conway, "Rectangular dielectric resonator antenna," *Electron. Lett.*, Vol. 19, No. 6, 218–219, 1983.
10. McAllister, M. W. and S. A. Long, "Resonant hemispherical dielectric antenna," *Electron. Lett.*, Vol. 20, No. 16, 657–659, 1984.

11. Mongia, R. K., A. Ittipiboon, P. Bhartia, and M. Cuhaci, "Electric-monopole antenna using a dielectric ring resonator," *Electron. Lett.*, Vol. 29, No. 17, 1530–1531, 1993.
12. Ittipiboon, A., R. K. Mongia, Y. M. M. Antar, P. Bhartia, and M. Cuhaci, "Aperture fed rectangular and triangular dielectric resonators for use as magnetic dipole antennas," *Electron. Lett.*, Vol. 29, No. 23, 2001–2002, 1993.
13. Leung, K. W., K. M. Luk, and E. K. N. Yung, "Spherical cap dielectric resonator antenna using apertue coupling," *Electron. Lett.*, Vol. 30, No. 17, 1366–1367, 1994.
14. Kishk, A. A., B. Ahn, and D. Kajfez, "Broadband stacked dielectric resonator antennas," *Electron. Lett.*, Vol. 25, No. 18, 1232–1233, 1989.
15. Kranenburg, R. A. and S. A. Long, "Microstrip transmission line excitation of dielectric resonator antennas," *Electron. Lett.*, Vol. 24, No. 18, 1156–1157, 1988.
16. Kranenburg, R. A., S. A. Long, and J. T. Williams, "Coplanar waveguide excitation of dielectric resonator antennas," *IEEE Trans. Antennas Propag.*, Vol. 39, No. 1, 119–122, 1991.
17. Zhou, G., A. A. Kishk, and A. W. Glisson, "Input impedance of a hemispherical dielectric resonator antenna excited by a coaxial probe," *Proc. IEEE Antennas Propag. Soc. Int. Symp. Ann Arbor, MI, USA*, Vol. 2, 1038–1041, 1993.
18. Shum, S. M. and K. M. Luk, "Stacked annular ring dielectric resonator antenna excited by axi-symmetric coaxial probe," *IEEE Trans. Antennas Propag.*, Vol. 43, No. 8, 889–892, 1995.
19. St-Martin, J. T. H., Y. M. M. Antar, A. A. Kishk, A. Ittipiboon, and M. Cuhaci, "Aperture-coupled dielectric resonator antenna," *Antennas Propag. Soc. Symp. 1991 Dig. London, Ontario, Canada*, Vol. 2, 1086–1089, 1991.
20. Antar, Y. M. M. and Z. Fan, "Theoretical investigation of aperture-coupled rectangular dielectric resonator antenna," *IEE Proc. — Microwaves, Antennas Propag.*, Vol. 143, No. 2, 113–118, 1996.
21. Mongia, R. K., A. Ittipiboon, Y. M. M. Antar, P. Bhartia, and M. Cuhaci, "A half-split cylindrical dielectric resonator antenna using slot-coupling," *IEEE Microw. Guid. Wave Lett.*, Vol. 3, No. 2, 38–39, 1993.
22. Glisson, A. W., D. Kajfez, and J. James, "Evaluation of modes in dielectric resonators using a surface integral equation formulation," *IEEE Trans. Microw. Theory Tech.*, Vol. 31, No. 12, 1023–1029, 1983.
23. Kajfez, D., A. W. Glisson, and J. James, "Computed modal field distributions for isolated dielectric resonators," *IEEE Trans. Microw.*, Vol. 32, No. 12, 1609–1616, 1984.
24. Kishk, A. A., A. W. Glisson, and D. Kajfez, "Computed resonant frequency and far fields of isolated dielectric discs," *Proc. IEEE Antennas Propag. Soc. Int. Symp. Ann Arbor, MI, USA*, Vol. 1, 408–411, 1993.
25. Mongia, R. K., A. Ittipiboon, and M. Cuhaci, "Measurement of radiation efficiency of dielectric resonator antennas," *IEEE Microw. Guid. Wave Lett.*, Vol. 4, No. 3, 80–82, 1994.
26. Kishk, A. A., H. A. Auda, and B. C. Ahn, "Radiation characteristics of cylindrical dielectric resonator antennas with new applications," *IEEE Antennas Propag. Soc. Newsl.*, Vol. 31, No. 1, 6–16, 1989.
27. Mongia, R. K. and P. Bhartia, "Dielectric resonator antennas — A review and general design relations for resonant frequency and bandwidth," *Int. J. Microw. Millimeter-Wave Comput. Eng.*, Vol. 4, No. 3, 230–247, 1994.
28. Gotra, S., V. S. Pandey, and R. S. Yaduvanshi, "A wideband graphene coated dielectric resonator antenna with circular polarization generation technique for THz applications," *Superlattices Microstruct.*, Vol. 150, No. June 2020, 106754, 2020.
29. Zhou, H., X. Chen, D. S. Espinoza, A. Mickelson, and D. S. Filipovic, "Nanoscale optical dielectric rod antenna for on-chip interconnecting networks," *IEEE Trans. Microw. Theory Tech.*, Vol. 59, No. 10, Part 2, 2624–2632, 2011.
30. Luk, K. M. and K. W. Leung, *Dielectric Resonator Antennas*, Research Studies Press Ltd., England, 2003.
31. Petosa, A., *Dielectric Resonator Antenna Handbook*, Artech, 2007.

32. Biagioni, P., J. S. Huang, and B. Hecht, "Nanoantennas for visible and infrared radiation," *Reports Prog. Phys.*, Vol. 75, No. 2, 40, 2012.
33. Walther, M., D. G. Cooke, C. Sherstan, M. Hajar, M. R. Freeman, and F. A. Hegmann, "Terahertz conductivity of thin gold films at the metal-insulator percolation transition," *Phys. Rev. B — Condens. Matter Mater. Phys.*, Vol. 76, No. 12, 1–9, 2007.
34. Varshney, G., S. Gotra, J. Kaur, V. S. Pandey, and R. S. Yaduvanshi, "Obtaining the circular polarization in a nano-dielectric resonator antenna for photonics applications," *Semicond. Sci. Technol.*, Vol. 34, No. 7, 07LT01, 2019.
35. Sethi, W. T., H. Vettikalladi, H. Fathallah, and M. Himdi, "Nantenna for standard 1550 nm optical communication systems," *Int. J. Antennas Propag.*, Vol. 2016, No. July, 1–9, 2016.
36. Varshney, G., S. Gotra, V. S. Pandey, and R. S. Yaduvanshi, "Proximity-coupled two-port multi-input-multi-output graphene antenna with pattern diversity for THz applications," *Nano Commun. Netw.*, Vol. 21, 2019.
37. Gotra, S., R. Yadav, and V. S. Pandey, "Beam reconfigurable graphene-based Yagi-Uda antenna with higher-order TM mode generation for THz applications," *Opt. Eng.*, Vol. 59, No. 11, 1–10, 2020.
38. Anagnostou, D. E., D. Torres, T. S. Teeslink, and N. Sepulveda, "Vanadium dioxide for reconfigurable antennas and microwave devices: Enabling RF reconfigurability through smart materials," *IEEE Antennas Propag. Mag.*, Vol. 62, No. 3, 58–73, 2020.
39. Hou, D., Y. Z. Xiong, W. Hong, W. L. Goh, and J. Chen, "Silicon-based on-chip antenna design for millimeter-wave/THz applications," *2011 IEEE Electrical Design of Advanced Packaging and Systems Symposium, EDAPS 2011*, 1–4, 2011.
40. Silveria, G., G. Wiederhecker, and H. Figueroa, "Dielectric resonator antenna for applications in nanophotonics," *Opt. Express*, Vol. 21, No. 1, 1234–1239, 2013.
41. Zou, L., et al., "Efficiency and scalability of dielectric resonator antennas at optical frequencies," *IEEE Photonics J.*, Vol. 6, No. 4, 1–10, 2014.
42. Zou, L., et al., "Dielectric resonator nanoantennas at visible frequencies," *Opt. Express*, Vol. 21, No. 1, 1344, 2013.
43. Leung, K. W., Y. M. Pan, X. S. Fang, E. H. Lim, K. M. Luk, and H. P. Chan, "Dual-function radiating glass for antennas and light covers — Part I: Omnidirectional glass dielectric resonator antennas," *IEEE Trans. Antennas Propag.*, Vol. 61, No. 2, 578–586, 2013.
44. Wang, S., L. Guo, and K. W. Leung, "Glass dielectric resonator antenna with inner 3D engraved pattern," *2019 Int. Symp. Antennas Propag. (ISAP)*, 1–3, Xi'an, China, 2019.
45. Pozar, D. M., *Microwave Engineering*, 4th Edition, Johan Wiley & Sons, Inc., 2005.
46. Yaduvanshi, R. S. and H. Parthasarathy, *Rectangular Dielectric Resonator Antennas*, 2015.
47. Van Bladel, J., "On the resonances of a dielectric resonator of very high permittivity," *IEEE Trans. Microw. Theory Tech.*, Vol. 23, No. 2, 199–208, 1975.
48. Mongia, R. K. and A. Ittipiboon, "Theoretical and experimental investigations on rectangular dielectric resonator antennas," *IEEE Trans. Antennas Propag.*, Vol. 45, No. 9, 1348–1356, 1997.
49. Mongia, R. K., "Theoretical and experimental resonant frequencies of rectangular dielectric resonators," *IEE Proc. H Microwaves, Antennas Propag.*, Vol. 139, No. 1, 98–104, 2010.
50. Mukherjee, B., P. Patel, and J. Mukherjee, "A review of the recent advances in dielectric resonator antennas," *Journal of Electromagnetic Waves and Applications*, Vol. 34, No. 9, 1095–1158, 2020.
51. Ullah, U., M. F. Ain, and Z. A. Ahmad, "A review of wideband circularly polarized dielectric resonator antennas," *China Commun.*, Vol. 14, No. 6, 65–79, 2017.
52. Dash, S. K. K., T. Khan, and Y. M. M. Antar, "A state-of-art review on performance improvement of dielectric resonator antennas," *Int. J. RF Microw. Comput. Eng.*, Vol. 28, No. 6, 2018.
53. Petosa, A. and A. Ittipiboon, "Dielectric resonator antennas: A historical review and the current state of the art," *IEEE Antennas Propag. Mag.*, Vol. 52, No. 5, 91–116, 2010.

54. Keyrouz, S. and D. Caratelli, "Dielectric resonator antennas: basic concepts, design guidelines, and recent developments at millimeter-wave frequencies," *Int. J. Antennas Propag.*, Vol. 2016, Article ID 6075680, 2016.
55. Luk, K. M., K. W. Leung, and K. Y. Chow, "Bandwidth and gain enhancement of a dielectric resonator antenna with the use of a stacking element," *Microw. Opt. Technol. Lett.*, Vol. 14, No. 4, 215–217, 1997.
56. Rao, Q., T. A. Denidni, and A. R. Sebak, "Broadband compact stacked T-shaped DRA with equilateral-triangle cross sections," *IEEE Microw. Wirel. Components Lett.*, Vol. 16, No. 1, 7–9, 2006.
57. Rocha, H., et al., "Bandwidth enhancement of stacked dielectric resonator antennas excited by a coaxial probe: An experimental and numerical investigation," *IET Microwaves, Antennas Propag.*, Vol. 2, No. 6, 580–587, 2008.
58. Liu, Y., H. Liu, M. Wei, and S. Gong, "A low-profile and high-permittivity dielectric resonator antenna with enhanced bandwidth," *IEEE Antennas Propag. Lett.*, Vol. 14, 791–794, 2015.
59. Al-Azza, A. A., N. A. Malalla, F. J. Harackiewicz, and K. Han, "Stacked conical-cylindrical hybrid dielectric resonator antenna for improved ultrawide bandwidth," *Progress In Electromagnetics Research Letters*, Vol. 79, 79–86, 2018.
60. Wong, K. L., N. C. Chen, and H. T. Chen, "Analysis of a hemispherical dielectric resonator antenna with an airgap," *IEEE Microw. Guid. Wave Lett.*, Vol. 3, No. 9, 355–357, 1993.
61. Chang, T. and J. Kiang, "Bandwidth broadening of dielectric resonator," *IEEE Trans. Antennas Propag.*, Vol. 57, No. 10, 205–207, 2009.
62. Khalily, M., M. K. A. Rahim, and A. A. Kishk, "Bandwidth enhancement and radiation characteristics improvement of rectangular dielectric resonator antenna," *IEEE Antennas Wirel. Propag. Lett.*, Vol. 10, 393–395, 2011.
63. Coulibaly, Y., M. Nedil, T. Denidni, and L. Talbi, "Design of a single circular soft surface applied to an aperture fed dielectric resonator antenna for gain and bandwidth improvement," *IEEE Antennas Propag. Soc. AP-S Int. Symp.*, 1692–1695, 2011.
64. Sahu, B., P. Tripathi, R. Singh, and S. P. Singh, "Simulation study of dielectric resonator antenna with metamaterial for improvement of bandwidth and gain," *IEEE MTT-S Int. Microw. RF Conf.*, 1–4, 2013.
65. Sahu, B., M. Aggarwal, P. Tripathi, and R. Singh, "Stacked cylindrical dielectric resonator antenna with metamaterial as a superstrate for enhancing the bandwidth and gain," *2013 IEEE Int. Conf. Signal Process. Comput. Control. ISPCC 2013*, 4–7, 2013.
66. Rashidian, A. and D. M. Klymyshyn, "On the two segmented and high aspect ratio rectangular dielectric resonator antennas for bandwidth enhancement and miniaturization," *IEEE Trans. Antennas Propag.*, Vol. 57, No. 9, 2775–2780, 2009.
67. Kishk, A. A., A. W. Glisson, and G. P. Junker, "Bandwidth enhancement for split cylindrical dielectric resonator antennas," *Progress In Electromagnetics Research*, Vol. 33, 97–118, 2001.
68. Walsh, A. G., C. S. De Young, and S. A. Long, "An investigation of stacked and embedded cylindrical dielectric resonator antennas," *IEEE Antennas Wirel. Propag. Lett.*, Vol. 5, No. 1, 130–133, 2006.
69. Hsiao, F. R., C. Wang, K. L. Wong, and T. W. Chiou, "Broadband very-high-permittivity dielectric resonator antenna for WLAN application," *IEEE Antennas Propag. Soc. AP-S Int. Symp.*, Vol. 4, 490–493, 2002.
70. Leung, K. W. and H. K. Ng, "The slot-coupled hemispherical dielectric resonator antenna with a parasitic patch: Applications to the circularly polarized antenna and wide-band antenna," *IEEE Trans. Antennas Propag.*, Vol. 53, No. 5, 1762–1769, 2005.
71. Chang, T. and J. Kiang, "Bandwidth broadening of dielectric resonator antenna by merging adjacent bands," *IEEE Trans. Antennas Propag.*, Vol. 57, No. 10, 3316–3320, 2009.
72. Shum, S. M. and K. M. Luk, "Dielectric ring resonator antenna with an air gap," *Electron. Lett.*, Vol. 30, No. 4, 277–278, 1994.

73. Kishk, A. A., A. W. Glisson, G. P. Junker, W. M. Ave, and E. Segundo, "Bandwidth enhancement for split cylindrical dielectric resonator antennas," *Progress In Electromagnetics Research*, Vol. 33, 97–118, 2001.
74. Fakhte, S., H. Oraizi, L. Matekovits, and G. Dassano, "Cylindrical anisotropic dielectric resonator antenna with improved gain," *IEEE Trans. Antennas Propag.*, Vol. 65, No. 3, 1404–1409, 2017.
75. Kiran, S., K. Dash, T. Khan, B. K. Kanaujia, and N. Nasimuddin, "Wideband cylindrical dielectric resonator antenna operating in HEM11δ mode with improved gain: A study of superstrate and reflector plane," *Int. J. Antennas Propag.*, 1–11, 2017.
76. Fakhte, S., H. Oraizi, L. Matekovits, L. S. Member, L. Matekovits, and S. Member, "High gain rectangular dielectric resonator antenna using uniaxial material at fundamental mode," *IEEE Trans. Antennas Propag.*, Vol. 65, No. 1, 342–347, 2017.
77. Fakhte, S., H. Oraizi, and L. Matekovits, "Gain improvement of rectangular dielectric resonator antenna by engraving grooves on its side walls," *IEEE Antennas Wirel. Propag. Lett.*, Vol. 16, 2167–2170, 2017.
78. Hwang, Y., Y. P. Zhang, K. M. Luk, and E. K. N. Yung, "Gain-enhanced miniaturised rectangular dielectric resonator antenna," *Electron. Lett.*, Vol. 33, No. 5, 350–352, 1997.
79. Dutta, K., D. Guha, C. Kumar, and Y. M. M. Antar, "New approach in designing resonance cavity high-gain antenna using nontransparent conducting sheet as the superstrate," *IEEE Trans. Antennas Propag.*, Vol. 63, No. 6, 2807–2813, 2015.
80. Coulibaly, Y., M. Nedil, A. Hagras, D. Hammou, L. Talbi, and T. A. Denidni, "Comparative study of gain enhancement of a dielectric resonator antenna using three superstrates for millimeter-wave applications," *IEEE Antennas Propag. Soc. AP-S Int. Symp.*, 32–33, 2012.
81. Coulibaly, Y., M. Nedil, L. Talbi, and T. A. Denidni, "High gain cylindrical dielectric resonator with superstrate for broadband millimeter-wave underground mining communications," *2010 14th Int. Symp. Antenna Technol. Appl. Electromagn. Am. Electromagn. Conf. ANTEM/AMEREM 2010*, No. 1, 3–6, 2010.
82. Dash, S. K. K., T. Khan, B. K. Kanaujia, and Y. M. M. Antar, "Gain improvement of cylindrical dielectric resonator antenna using flat reflector plane: A new approach," *IET Microwaves, Antennas Propag.*, Vol. 11, No. 11, 1622–1628, 2017.
83. Dash, S. K. K. and T. Khan, "Wideband high gain conical dielectric resonator antenna: An experimental study of superstrate and reflector," *Int. J. RF Microw. Comput. Eng.*, Vol. 27, No. 9, 1–10, 2017.
84. Al-Hasan, M. J., T. A. Denidni, and A. R. Sebak, "Millimeter-wave EBG-based aperture-coupled dielectric resonator antenna," *IEEE Trans. Antenna Propag.*, Vol. 61, No. 8, 4354–4357, 2013.
85. Nasimuddin and K. P. Esselle, "Antennas with dielectric resonators and surface mounted short horns for high gain and large bandwidth," *IET Microwaves Antennas Propag. Microwaves Antennas Propag.*, Vol. 1, No. 3, 723–728, 2007.
86. Denidni, T. A., Y. Coulibaly, and H. Boutayeb, "Hybrid dielectric resonator antenna with circular mushroom-like structure for gain improvement," *IEEE Trans. Antennas Propag.*, Vol. 57, No. 4, 1043–1049, 2009.
87. Coulibaly, Y., H. Boutayeb, T. A. Denidni, and L. Talbi, "Gain enhancement of a dielectric resonator antenna using a cylindrical electromagnetic crystal substrate," *2007 IEEE Antennas and Propagation Society International Symposium*, 1325–1328, 2007.
88. Fakhte, S., H. Oraizi, and M. H. Vadjed Samiei, "A high gain dielectric resonator loaded patch antenna," *Progress In Electromagnetics Research C*, Vol. 30, 147–158, 2012.
89. Petosa, A. and S. Thirakoune, "Rectangular dielectric resonator antennas with enhanced gain," *IEEE Trans. Antennas Propag.*, Vol. 59, No. 4, 1385–1389, 2011.
90. Fakhte, S., H. Oraizi, and L. Matekovits, "High gain rectangular dielectric resonator antenna using uniaxial material at fundamental mode," *IEEE Trans. Antennas Propag.*, Vol. 65, No. 1, 342–347, 2017.

91. Verma, A. and G. Varshney, "Techniques of controlling bandwidth and gain of the dielectric resonator antenna," *Int. J. Emerg. Technol. Adv. Eng.*, Vol. 5, No. 1, 131–135, 2015.
92. Varshney, G., R. S. Yaduvanshi, and V. S. Pandey, "Gain and bandwidth controlling of dielectric slab rectangular dielectric resonator antenna," *12th IEEE International Conference Electronics, Energy, Environment, Communication, Computer, Control: (E3-C3), INDICON 2015*, Vol. 3, 6–9, 2016.
93. Fakhte, S., "A high gain dielectric resonator loaded patch antenna," *Progress In Electromagnetics Research C*, Vol. 30, 147–158, 2012.
94. Oliver, M. B., Y. M. M. Antar, R. K. Mongia, and A. Ittipiboon, "Circularly polarised rectangular dielectric resonator antenna," *Electron. Lett.*, Vol. 31, No. 6, 418–419, 1995.
95. Tam, M. T. K. and R. D. Murch, "Circularly polarized circular sector dielectric resonator antenna," *IEEE Trans. Antennas Propag.*, Vol. 48, No. 1, 126–128, 2000.
96. Fang, X. S., K. W. Leung, and D.-W. C. D. Resonator, "Linear-/circular-polarization designs of dual-/wide-band cylindrical dielectric resonator antennas," *IEEE Trans. Antennas Propag.*, Vol. 60, No. 6, 2662–2671, 2012.
97. Pan, Y., K. W. Leung, and E. H. Lim, "Compact wideband circularly polarized rectangular dielectric resonator antenna with dual underlaid hybrid coupler," *Microw. Opt. Technol. Lett.*, Vol. 52, No. 12, 2789–2791, 2010.
98. Lim, E. H., K. W. Leung, and X. S. Fang, "The compact circularly-polarized hollow rectangular dielectric resonator antenna with an underlaid quadrature coupler," *IEEE Trans. Antenna Propag.*, Vol. 59, No. 1, 288–293, 2011.
99. Zhang, M., B. Li, and X. Lv, "Cross-slot-coupled wide dual-band circularly polarized rectangular dielectric resonator antenna," *IEEE Antennas Wirel. Propag. Lett.*, Vol. 13, 532–535, 2014.
100. Pan, J. and M. Zou, "Wideband hybrid circularly polarised rectangular dielectric resonator antenna excited by modified cross-slot," *Electron. Lett.*, Vol. 50, No. 16, 1123–1125, 2014.
101. Ding, Y., K. W. Leung, and K. M. Luk, "Compact circularly polarized dualband zonal-slot/DRA hybrid antenna without external ground plane," *IEEE Trans. Antennas Propag.*, Vol. 59, No. 6, 2404–2409, 2011.
102. Zou, M., J. Pan, and Z. Nie, "A wideband circularly polarized rectangular dielectric resonator antenna excited by an archimedean spiral slot," *IEEE Antennas Wirel. Propag. Lett.*, Vol. 14, 446–449, 2015.
103. Varshney, G., V. S. Pandey, R. S. Yaduvanshi, and L. Kumar, "Wide band circularly polarized dielectric resonator antenna with stair-shaped slot excitation," *IEEE Trans. Antennas Propag.*, Vol. 65, No. 3, 1380–1383, 2017.
104. Varshney, G., S. Gotra, R. Singh, V. S. Pandey, and R. S. Yaduvanshi, "Dimensions selection criteria of stair-shaped slot for obtaining the wideband response of CPDRA," *Def. Sci. J.*, Vol. 69, No. 5, 442–447, 2019.
105. Khalily, M., M. R. Kamarudin, M. Mokayef, and M. H. Jamaluddin, "Omnidirectional circularly polarized dielectric resonator antenna for 5.2-GHz WLAN applications," *IEEE Antennas Wirel. Propag. Lett.*, Vol. 13, 443–446, 2014.
106. Pan, Y. and K. W. Leung, "Wideband circularly polarized trapezoidal dielectric resonator antenna," *IEEE Antennas Wirel. Propag. Lett.*, Vol. 9, 588–591, 2010.
107. Wang, K. X. and H. Wong, "A circularly polarized antenna by using rotated-stair dielectric resonator," *IEEE Antennas Wirel. Propag. Lett.*, Vol. 14, 787–790, 2015.
108. Khalily, M., M. R. Kamarudin, and M. H. Jamaluddin, "A novel square dielectric resonator antenna with two unequal inclined slits for wideband circular polarization," *IEEE Antennas Wirel. Propag. Lett.*, Vol. 12, 1256–1259, 2013.
109. Varshney, G., S. Gotra, V. S. Pandey, and R. S. Yaduvanshi, "The generation of circular polarization in cylindrical dielectric resonator antenna using an arc-shaped dielectric element," *IET Conf. Publ.*, Vol. 2018, No. CP741, 3–5, 2018.

110. Gotra, S., V. S. Pandey, and B. Singh, "Bandwidth enhancement technique of a dual-band circularly polarized dielectric resonator antenna," *Indian J. Pure Appl. Phys.*, Vol. 59, No. March, 229–232, 2021.
111. Long, R. T., R. J. Dorris, S. A. Long, M. A. Khayat, and J. T. Williams, "Use of parasitic strip to produce circular polarisation and increased bandwidth for cylindrical dielectric resonator antenna," *Electron. Lett.*, Vol. 37, No. 7, 406–408, 2001.
112. Varshney, G., S. Gotra, V. S. Pandey, and R. S. Yaduvanshi, "Inverted-sigmoid shaped multiband dielectric resonator antenna with dual-band circular polarization," *IEEE Trans. Antennas Propag.*, Vol. 66, No. 4, 2067–2072, 2018.
113. Pan, Y. M. and K. W. Leung, "Wideband omnidirectional circularly polarized dielectric resonator antenna with parasitic strips," *IEEE Trans. Antennas Propag.*, Vol. 60, No. 6, 2992–2997, 2012.
114. Varshney, G., V. S. Pandey, and R. S. Yaduvanshi, "Axial ratio bandwidth enhancement of a circularly polarized rectangular dielectric resonator antenna," *Int. J. Microw. Wirel. Technol.*, Vol. 10, No. 8, 984–990, 2018.
115. Gotra, S., G. Varshney, R. S. Yaduvanshi, and V. S. Pandey, "Dual-band circular polarisation generation technique with the miniaturisation of a rectangular dielectric resonator antenna," *IET Microwaves, Antennas Propag.*, Vol. 13, No. 10, 1742–1748, 2019.
116. Lee, J. M., et al., "'Circularly polarized semi-eccentric annular dielectric resonator antenna for X-band applications," *IEEE Antennas Wirel. Propag. Lett.*, Vol. 14, 1810–1813, 2015.
117. Fakhte, S., H. Oraizi, and R. Karimian, "A novel low-cost circularly polarized rotated stacked dielectric resonator antenna," *IEEE Antennas Wirel. Propag. Lett.*, Vol. 13, 722–725, 2014.
118. Fakhte, S., H. Oraizi, R. Karimian, and R. Fakhte, "A new wideband circularly polarized stair-shaped dielectric resonator antenna," *IEEE Trans. Antennas Propag.*, Vol. 63, No. 4, 1828–1832, 2015.
119. Pan, Y. M., K. W. Leung, and K. Lu, "Omnidirectional linearly and circularly polarized rectangular dielectric resonator antennas," *IEEE Trans. Antennas Propag.*, Vol. 60, No. 2, Part 2, 751–759, 2012.
120. Lu, K., K. W. Leung, and Y. M. Pan, "Theory and experiment of the hollow rectangular dielectric resonator antenna," *IEEE Antennas Wirel. Propag. Lett.*, Vol. 10, 631–634, 2011.
121. Sulaiman, M. I. and S. K. Khamas, "A singly fed rectangular dielectric resonator antenna with a wideband circular polarization," *IEEE Antennas Wirel. Propag. Lett.*, Vol. 9, 615–618, 2010.
122. Sulaiman, M. I. and S. K. Khamas, "A singly fed wideband circularly polarized dielectric resonator antenna using concentric open half-loops," *IEEE Antennas Wirel. Propag. Lett.*, Vol. 10, 1305–1308, 2011.
123. Zou, M., J. Pan, and Z. Nie, "A wideband circularly polarized rectangular dielectric resonator antenna excited by an archimedean spiral slot," *IEEE Antennas Wirel. Propag. Lett.*, Vol. 14, 446–449, 2015.
124. Chair, R., S. L. S. Yang, A. A. Kishk, K. F. Lee, and K. M. Luk, "Aperture fed wideband circularly polarized rectangular stair shaped dielectric resonator antenna," *IEEE Trans. Antennas Propag.*, Vol. 54, No. 4, 1350–1352, Apr. 2006.
125. Pan, Y., K. W. Leung, and E. H. Lim, "Compact wideband circularly polarized rectangular dielectric resonator antenna with dual underlaid hybrid couplers," *Microw. Opt. Technol. Lett.*, Vol. 52, No. 12, 2789–2791, 2010.
126. Tam, M. T. K. and R. D. Murch, "Half volume dielectric resonator antenna designs," *Electron. Lett.*, Vol. 33, No. 23, 1914–1916, 1997.
127. Keefe, S. G. O., S. P. Kingsley, and S. Saario, "FDTD simulation of radiation characteristics dielectric resonator antennas," *IEEE Trans. Antenna Propag.*, Vol. 50, No. 2, 175–179, 2002.
128. Rashidian, A. and L. Shafai, "Compact lightweight polymeric-metallic resonator antennas using a new radiating mode," *IEEE Trans. Antennas Propag.*, Vol. 64, No. 1, 16–24, 2016.

129. Iqbal, A., A. Bouazizi, S. Kundu, I. Elfergani, and J. Rodriguez, "Dielectric resonator antenna with top loaded parasitic strip elements for dual-band operation," *Microw. Opt. Technol. Lett.*, Vol. 61, No. 9, 2134–2140, 2019.
130. Mongia, R. K., A. Ittibipoon, and M. Cuhaci, "Low profile dielectric resonator antennas using a very high permittivity material," *Electron. Lett.*, Vol. 30, No. 17, 1362–1363, 1994.
131. Rashidian, A., S. Member, L. Shafai, and L. Fellow, "Miniaturized transparent metallodielectric resonator antennas integrated with amorphous silicon solar cells," *IEEE Trans. Antennas Propag.*, Vol. 65, No. 5, 2265–2275, 2017.
132. Sharma, A., A. Sarkar, A. Biswas, and M. J. Akhtar, "A-shaped wideband dielectric resonator antenna for wireless communication systems and its MIMO implementation," *Int. J. RF Microw. Comput. Eng.*, Vol. 28, No. 8, 1–9, 2018.
133. Sharma, A. and A. Biswas, "Wideband multiple-input-multiple-output dielectric resonator antenna," *IET Microwaves, Antennas Propag.*, Vol. 11, No. 4, 496–502, 2017.
134. Aqeel, S., et al., "A dual-band multiple input multiple output frequency agile antenna for GPSL1/Wi-Fi/WLAN2400/LTE applications," *Int. J. Antennas Propag.*, Vol. 2016, 1–11, 2016.
135. Roslan, S. F., M. R. Kamarudin, M. Khalily, and M. H. Jamaluddin, "An MIMO rectangular dielectric resonator antenna for 4G applications," *IEEE Antennas Wirel. Propag. Lett.*, Vol. 13, 321–324, 2014.
136. Sharawi, M. S., S. K. Podilchak, M. U. Khan, and Y. M. Antar, "Dual-frequency DRA-based MIMO antenna system for wireless access points," *IET Microwaves, Antennas Propag.*, Vol. 11, No. 8, 1174–1182, 2017.
137. Trivedi, K. and D. Pujara, "Mutual coupling reduction in wideband tree shaped fractal dielectric resonator antenna array using defected ground structure for MIMO applications," *Microw. Opt. Technol. Lett.*, Vol. 59, No. 11, 2735–2742, 2017.
138. Das, G., A. Sharma, and R. K. Gangwar, "Wideband self-complementary hybrid ring dielectric resonator antenna for MIMO applications," *IET Microwaves, Antennas Propag.*, Vol. 12, No. 1, 108–114, 2017.
139. Abedian, M., S. K. A. Rahim, C. Fumeaux, S. Danesh, Y. C. Lo, and M. H. Jamaluddin, "Compact ultrawideband MIMO dielectric resonator antennas with WLAN band rejection," *IET Microwaves, Antennas Propag.*, Vol. 11, No. 11, 1524–1529, 2017.
140. Gotra, S., G. Varshney, V. S. Pandey, and R. S. Yaduvanshi, "Super-wideband multi-input-multi-output dielectric resonator antenna," *IET Microwaves, Antennas Propag.*, Vol. 14, No. 1, 21–27, 2020.
141. Sharawi, M. S. and E. Rajo-iglesias, "Printed multi-band MIMO antenna systems and their performance metrics," *IEEE Antennas Propag. Mag.*, Vol. 55, No. 5, 218–232, 2013.
142. Hu, Y., Y. M. Pan, and M. D. Yang, "Circularly polarized MIMO dielectric resonator antenna with reduced mutual coupling," *IEEE Trans. Antennas Propag.*, Vol. 69, No. 7, 3811–3820, 2021.
143. Iqbal, J., U. Illahi, M. I. Sulaiman, M. M. Alam, M. M. Suud, and M. N. Mohd Yasin, "Mutual coupling reduction using hybrid technique in wideband circularly polarized MIMO Antenna for WiMAX Applications," *IEEE Access*, Vol. 7, 40951–40958, 2019.
144. Varshney, G., R. Singh, V. S. Pandey, and R. S. Yaduvanshi, "Circularly polarized two-port MIMO dielectric resonator antenna," *Progress In Electromagnetics Research M*, Vol. 91, 19–28, 2020.
145. Kumar, N., S. Gourab, D. Ravi, and K. Gangwar, "L-shaped dielectric resonator based circularly polarized Multi-Input-Multi-Output (MIMO) antenna for Wireless Local Area Network (WLAN) applications," *Int. J. RF Microw. Comput. Eng.*, 1–11, 2018.
146. Chen, H. N., J. M. Song, and J. D. Park, "A compact circularly polarized MIMO dielectric resonator antenna over electromagnetic band-gap surface for 5G applications," *IEEE Access*, Vol. 7, 140889–140898, 2019.
147. Zou, L. and C. Fumeaux, "A cross-shaped dielectric resonator antenna for multifunction and polarization diversity applications," *IEEE Antennas Wirel. Propag. Lett.*, Vol. 10, 742–745, 2011.

148. Das, G., N. K. Sahu, and R. K. Gangwar, "Pattern diversity based double sided dielectric resonator antenna for MIMO applications," *2018 IEEE Indian Conf. Antennas Propagation, InCAP 2018*, 1–4, 2018.
149. Das, G., A. Sharma, and R. K. Gangwar, "Dielectric resonator based circularly polarized MIMO antenna with polarization diversity," *Microw. Opt. Technol. Lett.*, Vol. 60, No. 3, 685–693, 2018.
150. Varshney, G., S. Gotra, S. Chaturvedi, V. S. Pandey, and R. S. Yaduvanshi, "Compact four-port MIMO dielectric resonator antenna with pattern diversity," *IET Microwaves, Antennas Propag.*, Vol. 13, No. 12, 2193–2198, 2019.
151. Das, G., N. K. Sahu, A. Sharma, R. K. Gangwar, and M. S. Sharawi, "FSS-based spatially decoupled back-to-back four-port MIMO DRA with multidirectional pattern diversity," *IEEE Antennas Wirel. Propag. Lett.*, Vol. 18, No. 8, 1552–1556, 2019.
152. Abdalrazik, A., A. S. A. El-Hameed, and A. B. Abdel-Rahman, "A three-port MIMO dielectric resonator antenna using decoupled modes," *IEEE Antennas Wirel. Propag. Lett.*, Vol. 16, 3104–3107, 2017.
153. Tian, R. T. R., V. Plicanic, B. K. L. B. K. Lau, and Z. Y. Z. Ying, "A compact six-port dielectric resonator antenna array: MIMO channel measurements and performance analysis," *IEEE Trans. Antennas Propag.*, Vol. 58, No. 4, 1369–1379, 2010.
154. Sharma, A. and A. Biswas, "Wideband multiple-input-multiple-output dielectric resonator antenna," *IET Microwaves, Antennas Propag.*, Vol. 11, No. 4, 496–502, 2017.
155. Headland, D., et al., "Terahertz magnetic mirror realized with dielectric resonator antennas," *Adv. Mater.*, Vol. 27, No. 44, 7137–7144, 2015.
156. Hosseininejad, S. E., et al., "Terahertz dielectric resonator antenna coupled to graphene plasmonic dipole," *12th European Conference on Antennas and Propagation (EuCAP 2018)*, 1–5, London, UK, 2018.
157. Varshney, G., "Tunable terahertz dielectric resonator antenna," *Silicon*, Vol. 13, No. 6, 1907–1915, 2020.
158. Iizuka, H., N. Engheta, H. Fujikawa, and K. Sato, "Arm-edge conditions in plasmonic folded dipole nanoantennas," *Opt. Express*, Vol. 19, No. 13, 12325, 2011.
159. Chen, P. and M. Farhat, "Modulatable optical radiators and metasurfaces based on quantum nanoantennas," *Phys. Rev. B*, Vol. 91, No. 035426, 1–8, 2015.
160. Sethi, W. T., H. Vettikalladi, and H. Fathallah, "Dielectric resonator nanoantenna at optical frequencies," *2015 Int. Conf. Inf. Commun. Technol. Res. ICTRC 2015*, 132–135, 2015.
161. Malheiros-Silveira, G. N., G. S. Wiederhecker, and H. E. Hernández-Figueroa, "Dielectric resonator antenna for applications in nanophotonics," *Opt. Express*, Vol. 21, No. 1, 1234, 2013.
162. Fumeaux, C., et al., "Terahertz and optical dielectric resonator antennas: Potential and challenges for efficient designs," *2016 10th European Conference on Antennas and Propagation, EuCAP 2016*, 2–5, 2016.
163. Chen, P. Y. and M. Farhat, "Modulatable optical radiators and metasurfaces based on quantum nanoantennas," *Phys. Rev. B — Condens. Matter Mater. Phys.*, Vol. 91, No. 3, 1–8, 2015.
164. Gotra, S., R. Yadav, V. S. Pandey, and R. S. Yaduvanshi, "Axial-ratio tuning in nano-dielectric resonator antenna for optical band applications," *2020 14th Eur. Conf. Antennas Propag. (EuCAP)*, 1–4, Copenhagen, Denmark, 2020.
165. Rui, G., R. L. Nelson, and Q. Zhan, "Circularly polarized unidirectional emission via a coupled plasmonic spiral antenna," *Opt. Lett.*, Vol. 36, No. 23, 4533, 2011.
166. Troubat, M., et al., "Mutual synthesis of combined microwave circuits applied to the design of a filter-antenna subsystem," *IEEE Trans. Microw. Theory Tech.*, Vol. 55, No. 6, 1182–1189, 2007.
167. Saraereh, O. A. and A. Iqbal, "Design of compact and miniaturize asymmetric SIR-DRA filter-antenna subsystem," *Journal of Electromagnetic Waves and Applications*, Vol. 30, No. 16, 2174–2184, 2016.
168. Lim, E. H. and K. W. Leung, "Use of the dielectric resonator antenna as a filter element," *IEEE Trans. Antennas Propag.*, Vol. 56, No. 1, 5–10, 2008.

169. Naeem, U., A. Iqbal, M. F. Shafique, and S. Bila, "Efficient design methodology for a complex DRA-SIW filter-antenna subsystem," *Int. J. Antennas Propag.*, Vol. 2017, 1–9, 2017.

170. Tang, H., C. Tong, and J. X. Chen, "Differential dual-polarized filtering dielectric resonator antenna," *IEEE Trans. Antennas Propag.*, Vol. 66, No. 8, 4298–4302, 2018.

171. Mallat, N. K. and A. Iqbal, "Out-of-band suppressed SIW-DRA based filter-antenna subsystem with flexible bandwidth and transmission zeros," *AEU — Int. J. Electron. Commun.*, Vol. 135, 153735, 2021.

172. Cook, B. S., J. R. Cooper, and M. M. Tentzeris, "Multi-layer RF capacitors on flexible substrates utilizing inkjet printed dielectric polymers," *IEEE Microw. Wirel. Components Lett.*, Vol. 23, No. 7, 353–355, 2013.

173. Yasin, A., F. U. Rehman, U. Naeem, S. A. Khan, and M. F. Shafique, "Top loaded TM01δ; mode cylindrical dielectric resonator for complex permittivity characterization of liquids," *Radioengineering*, Vol. 25, No. 4, 714–720, 2016.

174. Iqbal, A., A. Smida, O. A. Saraereh, Q. H. Alsafasfeh, N. K. Mallat, and B. M. Lee, "Cylindrical dielectric resonator antenna-based sensors for liquid chemical detection," *Sensors (Switzerland)*, Vol. 19, No. 5, 2–10, 2019.

175. Iqbal, A., A. J. Alazemi, and N. K. Mallat, "Slot-DRA-based independent dual-band hybrid antenna for wearable biomedical devices," *IEEE Access*, Vol. 7, 184029–184037, 2019.

176. Iqbal, A., M. I. Waly, A. Smida, and N. K. Mallat, "Dielectric resonator antenna with reconfigurable polarization states," *IET Microwaves, Antennas Propag.*, Vol. 15, No. 7, 683–690, 2021.